

AD-A107 634 NAVAL UNDERWATER SYSTEMS CENTER NEW LONDON CT NEW LO--ETC F/6 12/1
TWO-CHANNEL LINEAR-PREDICTIVE SPECTRAL ANALYSIS PROGRAM FOR THE--ETC(U)
OCT 81 A H NUTTALL

UNCLASSIFIED NUSC-TR-6533

NL

1 of 1
AD-A
07854

END
DATE
FILED
1-82
DTIC

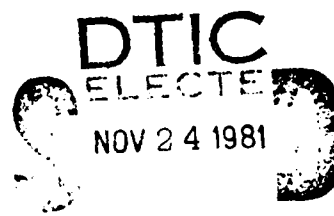
2
NUSC Technical Report 6533
1 October 1981

J.R.

AD A 107 634

Two-Channel Linear-Predictive Spectral Analysis; Program for the HP 9845 Desk Calculator

Albert H. Nuttall
Surface Ship Sonar Department



A

**Naval Underwater Systems Center
Newport, Rhode Island / New London, Connecticut**

DTIC FILE COPY

Approved for public release; distribution unlimited.

Preface

This research was conducted under NUSC Project No. A75205, Subproject No. ZR0000101, "Applications of Statistical Communication Theory to Acoustic Signal Processing"; Principal Investigator, Dr. A. H. Nuttall, Code 3302; Program Manager, CAPT D. F. Parrish, Naval Material Command, MAT 08L.

The Technical Reviewer for this report was Dr. P. B. Abraham, Code 3331.

REVIEWED AND APPROVED: 1 October 1981



**W. A. Von Winkle
Associate Technical Director
for Technology**

The author of this report is located at the New London Laboratory, Naval Underwater Systems Center, New London, Connecticut 06320.

REPORT DOCUMENTATION PAGE		READ INSTRUCTIONS BEFORE COMPLETING FORM	
1. REPORT NUMBER TR 6533	2. GOVT ACCESSION NO. AD-A107 634	3. RECIPIENT'S CATALOG NUMBER	
4. TITLE (and Subtitle) Two-Channel Linear-Predictive Spectral Analysis; Program for the HP 9845 Desk Calculator		5. TYPE OF REPORT & PERIOD COVERED	
7. AUTHOR(s) Albert H. Nuttall		6. PERFORMING ORG. REPORT NUMBER	
9. PERFORMING ORGANIZATION NAME AND ADDRESS Naval Underwater Systems Center New London Laboratory New London, Connecticut 06320		10. PROGRAM ELEMENT, PROJECT, TASK AREA & WORK UNIT NUMBERS A75205	
11. CONTROLLING OFFICE NAME AND ADDRESS Naval Material Command Headquarters Code 08L Washington, DC 20360		12. REPORT DATE 1 October 1981	
14. MONITORING AGENCY NAME & ADDRESS (if different from Controlling Office)		13. NUMBER OF PAGES 52	
		15. SECURITY CLASS. (of this report) Unclassified	
		15a. DECLASSIFICATION/DOWNGRADING SCHEDULE	
16. DISTRIBUTION STATEMENT (of this Report) Approved for public release; distribution unlimited.			
17. DISTRIBUTION STATEMENT (of the abstract entered in Block 20, if different from Report)			
18. SUPPLEMENTARY NOTES			
19. KEY WORDS (Continue on reverse side if necessary and identify by block number) Akaike Information Criterion Linear Prediction Autoregressive Process Short Data Segments Basic Program Spectral Analysis Coherence Estimation Tonal Interference Cross Spectra			
20. ABSTRACT (Continue on reverse side if necessary and identify by block number) A program for linear-predictive spectral analysis of two channels of data, including estimation of the auto-spectra, cross-spectrum, magnitude-squared-coherence, and the argument of the coherence, is presented in Basic for the HP 9845 desk calculator. Timing results for the major subroutines are included, and their dependence on the fundamental parameters of the data, filter, and desired spectral resolution is indicated. This technique and program for spectral analysis are very appropriate for short data segments. In particular, a positive-definite spectral matrix estimate is guaranteed.			

20. Abstract (Cont'd)

→ Applications to examples including a strong tonal interference in one channel are made, and a possible shortcoming of the technique is pointed out. A suggested remedy is proposed and a philosophy for multichannel spectral analysis is suggested for further consideration. ←



Table of Contents

	Page
List of Illustrations	i
List of Tables	ii
List of Symbols	iii
Introduction	1
Use of Program for Spectral Analysis	2
Application to Processes with Tones	5
Discussion and Conclusions	23
Appendix A - Program for Two-Channel Linear-Predictive Spectral Analysis	A-1
Appendix B - General Filter and Spectral Relations	B-1
References	R-1

List of Illustrations

Figure		Page
1	True Spectral Characteristics With No Tone	6
2	Spectral Estimates for $N = 100$, $P_{max} = 15$, $P_{best} = 1$, No Tone	7
3	Spectral Estimates for $N = 100$, $P_{max} = 15$, $P_{best} = 1$, Tone Power = -32.9 dB	9
4	Spectral Estimates for $N = 100$, $P_{max} = 15$, $P_{best} = 4$, Tone Power = -26.9 dB	10
5	Spectral Estimates for $N = 100$, $P_{max} = 15$, $P_{best} = 8$, Tone Power = -20.8 dB	11
6	Spectral Estimates for $N = 100$, $P_{max} = 15$, $P_{best} = 8$, Tone Power = -14.8 dB	13
7	Spectral Estimates for $N = 100$, $P_{max} = 15$, $P_{best} = 8$, Tone Power = -8.8 dB	14
8	Spectral Estimates for $N = 1000$, $P_{max} = 8$, $P_{best} = 8$, Tone Power = -24.6 dB	15

List of Illustrations (Cont'd)

Figure		Page
9	Spectral Estimates for N = 1000, Pmax = 8, Pbest = 8, Tone Power = -18.6 dB	16
10	Spectral Estimates for N = 1000, Pmax = 8, Pbest = 8, Tone Power = -12.6 dB	17
11	Spectral Estimates for N = 1000, Pmax = 8, Pbest = 8, Tone Power = -6.6 dB	18
12	Spectral Estimates for N = 1000, Pmax = 8, Pbest = 8, Tone Power = -0.6 dB	19
13	Akaike Information Criterion for N = 1000, Tone Power = -12.6 dB	20
14	Auto-Spectral Estimates for Multitone Example, N = 64, P = 12	21
15	Spectral Estimates for Multitone Example, N = 64, P = 6	22
A-1	Spectral Estimates for N = 20, Pmax = 6, Pbest = 4	A-1

List of Tables

Table		Page
1	Execution Times for Subroutine Pcc	3
2	Execution Times for Subroutine Pfc	3
3	Execution Times for Subroutine Peftf	3
4	Execution Times for Subroutine Sdm	3
5	Execution Times for Subroutine Acm	4
6	Execution Times for Subroutine Fft10	4

List of Symbols

N	Number of data points in each process
Pmax	Maximum order of predictive filter to be considered
Nfft	Size of FFT to be used in spectral analysis
AIC	Akaike Information Criterion
Pbest	Best order of predictive filter to use, based on AIC
Δ	Time sampling increment
f	Frequency
f_N	Nyquist frequency, $(2\Delta)^{-1}$
$x_1(k)$	k-th sample of process 1
$x_2(k)$	k-th sample of process 2
$w_n(k)$	Additive white noise ($n = 1, 2$)
P	Predictive filter order
$A_P^{(P)}$	Partial forward correlation coefficient of order P
R_o	Covariance matrix at zero delay

Two-Channel Linear-Predictive Spectral Analysis; Program for the HP 9845 Desk Calculator

Introduction

Spectral analysis of short data segments by the standard FFT procedure is not a viable approach; unstable and/or coarse estimates of the spectra result. An attractive technique in this case is linear-predictive spectral analysis, both for the single-channel as well as the multiple-channel cases. See references 1-9, particularly references 7-9 which derive and give Fortran programs for a multiple-channel linear-predictive spectral analysis technique that is a generalization of Burg's technique for the single-channel case (reference 1).

The purpose of this report is twofold: first, we translate the Fortran program in reference 9 into Basic for use on the Hewlett-Packard HP 9845 Desk Calculator, and in the process, also make some minor improvements and modifications to the format and printout statements. We also limit consideration to the two-channel case and thereby take advantage of some simplifications in computing possible for this special case. Second, we apply the program to a pair of stationary processes, one of which has pure tones that are not present in the other process. In this manner, we point out a possibly deleterious effect on the auto-spectral estimates and the coherence estimate, and indicate a method for circumventing some of the difficulty. As a byproduct, a philosophy for multichannel spectral analysis is suggested for further consideration.

Use of Program For Spectral Analysis

In appendix A, the listing for the two-channel linear-predictive spectral analysis technique is presented. Inputs required of the user are the following:

N	Number of data points in each process
Pmax	Maximum order of predictive filter to be considered
Nfft	Size of FFT to be used in spectral computation. (1)

In addition to these integer inputs, the user must modify the subroutine SUB Data (N,X(*)) to accommodate and read in his particular two-channel data. All data are presumed real.

The program computes the (sample) means of each of the two processes and subtracts the means from the data. (Some possible ramifications of this procedure are considered in reference 6, appendix B; in addition, the effect of choosing too small an FFT size, Nfft, is discussed in reference 6.) Next, the covariance matrix (at zero delay) of the input data is computed, and the Akaike Information Criterion (AIC, reference 8, pages 42-44) is evaluated and used to select the integer

Pbest	Best order of predictive filter to use. (2)
-------	---

The forward and backward partial correlation coefficients (references 7-9) are evaluated through order Pmax, as well as the forward predictive filter coefficients for Pbest. The normalized correlation matrices are computed through Pmax (extrapolated values beyond Pbest) and the spectral density matrix is computed (via an FFT) from zero to Nyquist frequency, $f_N = (2\Delta)^{-1}$, where Δ is the time-sampling increment of the processes. A partial check on the adequacy of the FFT size, Nfft, is afforded by a printout of the areas under the spectral estimates and comparison with the (sample) covariances of the input data. Finally, the inverse FFT of the spectral estimate gives the aliased normalized correlation matrices; the motivation and equations for this approach are given in reference 9.

A sample printout for a short data sequence (20 data points in each process) is given after the program listing in appendix A, as a test or check case on a user-written program. Also, plots of the corresponding auto-spectral estimates and the coherence estimates are given there for completeness, although this example has no real physical significance.

Timing Results

Execution times for the five major subroutines,

Pcc	Partial correlation coefficients
Pfc	Predictive filter coefficients
Peftf	Predictive error filter transfer function
Sdm	Spectral density matrix
Acm	Aliased correlation matrices, (3)

are given in tables 1-5 below, for the HP 9845B Desk Calculator equipped with the Fast Processor Upgrade Kit. Only those variables utilized in each subroutine are considered in these tables, since execution time is independent of the other variables; for example, the execution time of subroutine Pcc does not depend on Pbest.

Table 1. Execution Times for Subroutine Pcc

N	Pmax	Seconds
20	6	1.9
50	10	5.4
100	5	4.7
100	10	9.5
100	15	14.1
1000	47	404.2

Table 2. Execution Times for Subroutine Pfc

Pmax	Pbest	Seconds
5	1	.09
10	1	.15
6	4	.24
15	5	.62
15	11	1.41
47	12	4.06

Table 3. Execution Times for Subroutine Peftf

Pbest	Nfft	Seconds
4	256	17.5
11	256	17.8
1	512	32.0
5	512	32.8
1	1024	63.9
11	1024	66.6

Table 4. Execution Times for Subroutine Sdm

Nfft	Seconds
256	8.9
512	17.7
1024	35.3

Table 5. Execution Times for Subroutine Acm

Nfft	Seconds
256	9.8
512	18.6
1024	37.7

From these tables, we are able to extract the following fairly accurate rules of thumb: the execution time of

- Pcc is linearly dependent on N and Pmax
- Pfc is linearly dependent on Pmax and Pbest
- Peftf is linearly dependent on Nfft, but is essentially independent of Pbest
- Sdm is linearly dependent on Nfft
- Acm is linearly dependent on Nfft. (4)

These rules allow extrapolation to other cases of interest to the user. The execution times of the FFT itself are given in table 6.

Table 6. Execution Times for Subroutine Fft10

Nfft	Seconds
128	2.6
256	4.5
512	8.4
1024	17.1

If the user is interested only in obtaining the predictive filter coefficients (for example, to do time domain prediction and signal processing), these results are available immediately after execution of subroutine Pfc. There is then no need to resort to the frequency domain routines that follow Pfc; in this manner, execution time and storage can be significantly reduced. An additional reduction in execution time is available by declaring all the loop counters in a subroutine to be INTEGER.

Application to Processes With Tones

Our first example is the two-channel case given numerically by the sample values in reference 7, page 17; reference 8, page K-12; and in reference 9, page D-18. The analytic expression for the autoregression is

$$\begin{aligned} x_1(k) &= .85 x_1(k-1) - .75 x_2(k-1) + w_1(k) \\ x_2(k) &= .65 x_1(k-1) + .55 x_2(k-1) + w_2(k) \end{aligned} \quad (5)$$

where $\{w_1(k)\}$ and $\{w_2(k)\}$ are uniformly distributed, independent white noise processes with zero means and variances $1/12$. General filter and spectral relations for moving-average and autoregressive processes are given in appendix B; these general relations are then specialized to this particular numerical example. It is shown in (B-31) et seq. that the auto spectrum of process $\{x_1(k)\}$ has *four poles and three zeros* in the finite z-plane, even though the two-channel recursion, (5), is only first-order regressive.

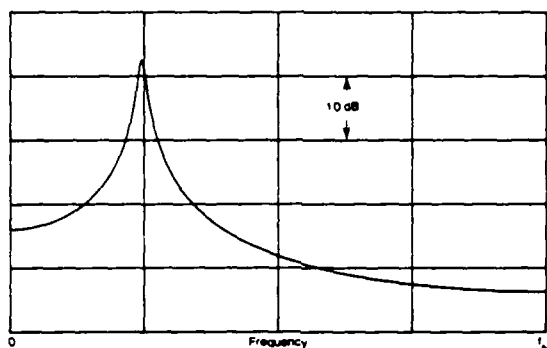
Generally, for a two-channel P-th order regression and independent white excitations (i.e., $E_k = 0$ for $k > P$, $F_k = I \delta_{k0}$, and $Q(z) = \Delta I$ in (B-18)), the auto- and cross-spectra of the processes each possess $4P$ poles and $3P$ zeros in the finite z-plane (of which P zeros occur at the origin). This is in contrast to the single-channel case, where $2P$ poles (and a P -th order zero only at the origin) can occur. This increased generality can be anticipated by the observation that whereas a single-channel approximation requires estimation of only P parameters, an M -channel approximation requires estimation of M^2P parameters ($4P$ for the two-channel case $M = 2$). Of course, for a fixed number, N , of data points from each process, the estimation of an increased number of parameters can only be done with increased variance; this is a manifestation of the tradeoff between resolution and stability that accompanies all spectral analysis techniques.

The first-order forward partial correlation coefficient for two-channel process (5) is

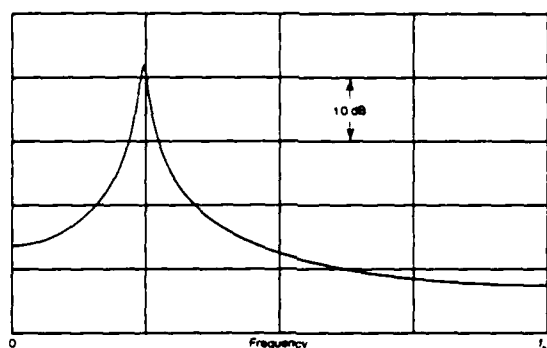
$$A_1^{(1)}(\text{true}) = \begin{bmatrix} .85 & -.75 \\ .65 & .55 \end{bmatrix}, \quad (6)$$

and all other higher-order coefficients are zero. The exact auto spectrum of the first process, $\{x_1(k)\}$, is shown (in dB) in figure 1A; the auto spectrum of the second process, $\{x_2(k)\}$, is shown in figure 1B; the magnitude-squared coherence is displayed in figure 1C; and the argument of the complex coherence or cross spectrum is depicted in figure 1D. There is seen to be a strong narrowband component at approximately one-fourth of the Nyquist frequency $f_N = (2\Delta)^{-1}$, where Δ is the time-sampling increment for the two-channel process (5). This leads to a peak magnitude-squared coherence value of .999013 at $2f\Delta = .2459$.

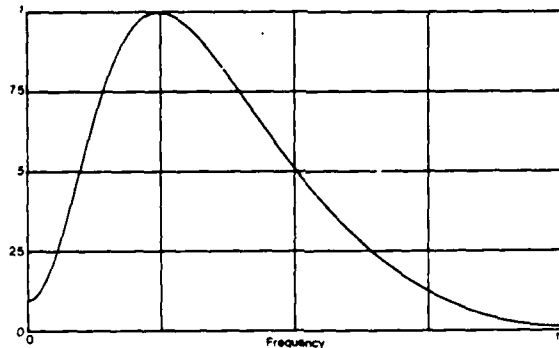
The results of applying the two-channel spectral analysis program in appendix A to the numerical data cited above, with $N = 100$, are shown in figure 2, where the



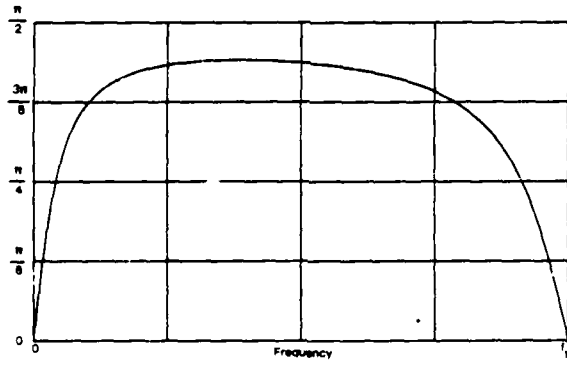
1A. Auto Spectrum of First Process



1B. Auto Spectrum of Second Process

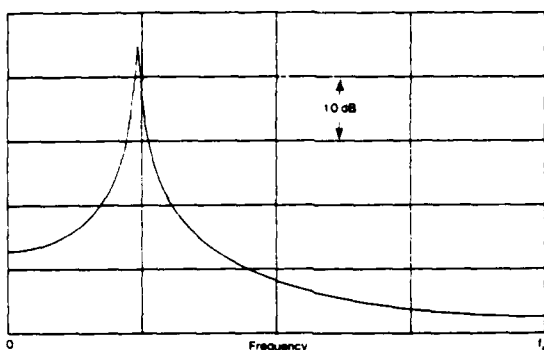


1C. Magnitude-Squared Coherence

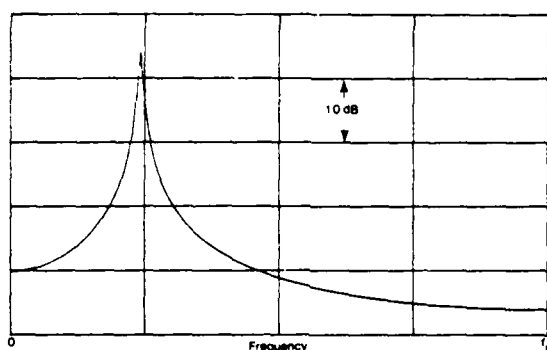


1D. Argument of Complex Coherence

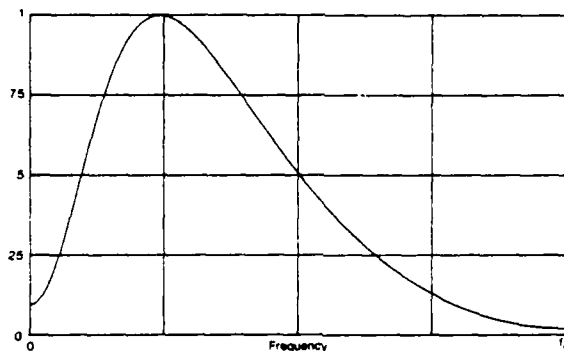
Figure 1. True Spectral Characteristics With No Tone



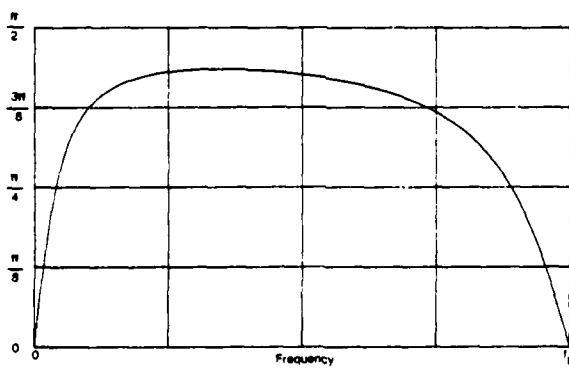
2A. Auto Spectrum of First Process



2B. Auto Spectrum of Second Process



2C. Magnitude-Squared Coherence



2D. Argument of Complex Coherence

Figure 2. Spectral Estimates for $N = 100$, $P_{max} = 15$, $P_{best} = 1$, No Tone

four parts of this figure correspond directly to those of figure 1. Pbest turns out to be equal to the correct value 1, and the spectral estimates are all quite good. In fact, the estimated magnitude-squared coherence reaches a peak value of .999745 versus the true value of .999013.

The covariance matrix of the process generated by (5) is (reference 8, page 18, after scaling by variance 1/12)

$$R_o(\text{true}) = \begin{bmatrix} 2.095 & 0.405 \\ 0.405 & 1.804 \end{bmatrix}. \quad (7)$$

The corresponding matrix estimate yielded by the program here, based on the particular $N = 100$ data values cited above, is

$$R_o = \begin{bmatrix} 4.62 & .916 \\ .916 & 3.80 \end{bmatrix} \text{ for } N = 100; \quad (8)$$

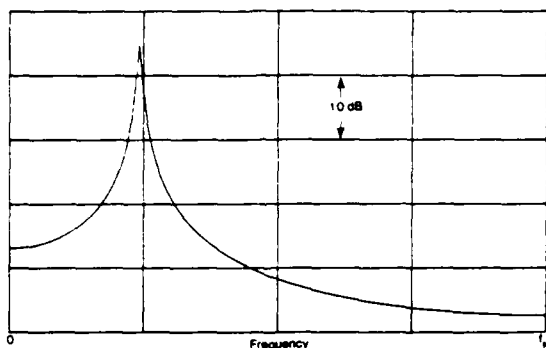
these values are approximately 2.2 times larger than (7), due to the fact that (5) is a narrowband process and the particular 100 pairs of samples used in the spectral estimates happen to lie on a local peak of the instantaneous waveforms. Although the local estimates of the absolute power levels are off considerably, the estimate of the forward partial correlation coefficient is very good; we find, instead of (6),

$$A_1^{(1)} = \begin{bmatrix} .872 & -.770 \\ .634 & .560 \end{bmatrix} \text{ for } N = 100. \quad (9)$$

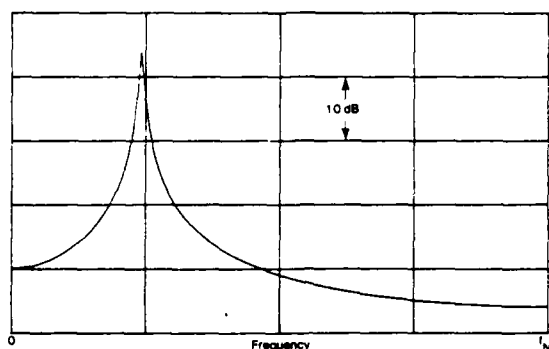
Next we add a pure tone only to the second process $\{x_2(k)\}$ at a frequency equal to 0.6 of the Nyquist frequency, i.e., at $0.6f_N$. The power in the tone is 1/512, i.e., 32.9 dB below the average power, 3.80, in this particular segment of autoregressive process $\{x_2(k)\}$; see (8). The resultant spectral estimates are shown in figure 3; they are virtually identical to figure 2. The only inadequacy of figure 3 is that the autospectral estimate in figure 3B gives no indication of the added tone; of course, there should ideally be no indication of the tone in figure 3A for the auto spectrum of $\{x_1(k)\}$. The value of Pbest was again 1, as determined by the AIC.

When the tonal power in the second process is increased to -26.9 dB, Pbest increases to 4 (see figure 4) and there are humps in both auto-spectral estimates near the tone frequency $0.6f_N$. The coherence estimates (magnitude and argument) are significantly perturbed in a considerable neighborhood of $0.6f_N$; this broad frequency-perturbation width is due to a small value of Pbest having been selected by the AIC.

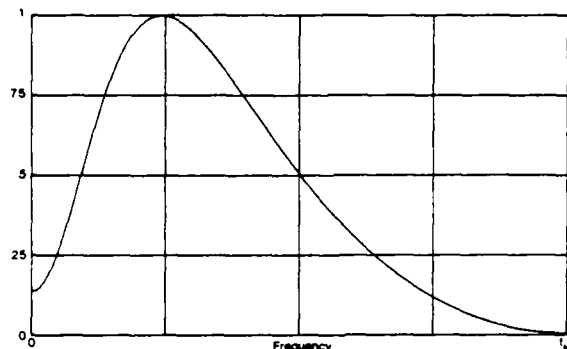
Increasing the tonal power to -20.8 dB results in the estimates depicted in figure 5. Now there is a considerable indication of the tonal power in figure 5B; however, there is also an *undesirable* indication in figure 5A at frequency $0.6f_N$ in the auto-spectral estimate for process $\{x_1(k)\}$. This "feed-across" is due to the fact that we are working with only $N = 100$ data samples of each process; with this small a data set, the "best" two-channel linear-prediction is misled into an erroneous indication. It is important to observe at this point that *any* auto-spectral estimate based on



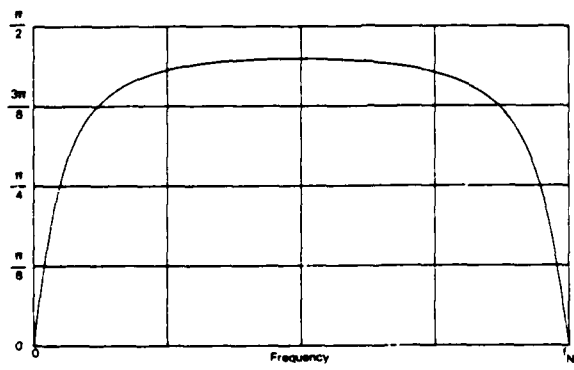
3A. Auto Spectrum of First Process



3B. Auto Spectrum of Second Process

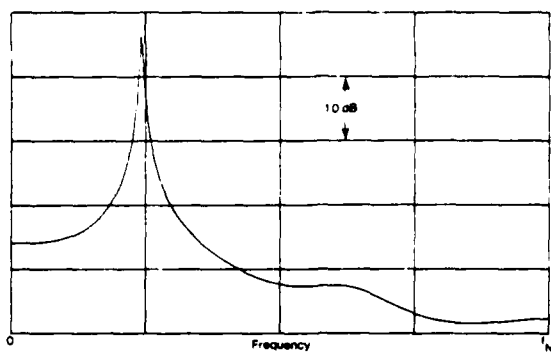


3C. Magnitude-Squared Coherence

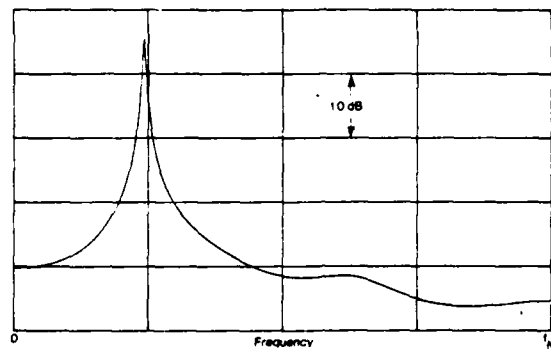


3D. Argument of Complex Coherence

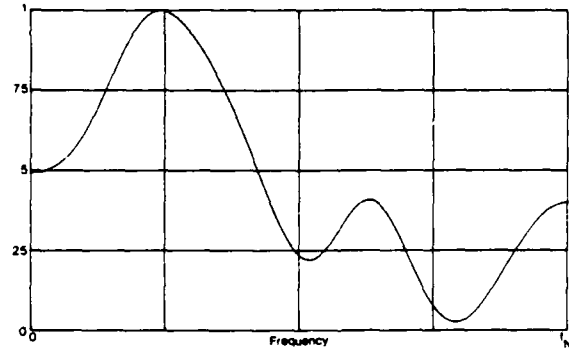
Figure 3. Spectral Estimates for $N = 100$, $P_{max} = 15$, $P_{best} = 1$, Tone Power = -32.9 dB



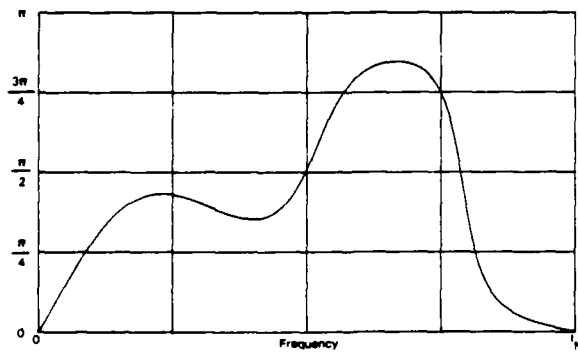
4A. Auto Spectrum of First Process



4B. Auto Spectrum of Second Process

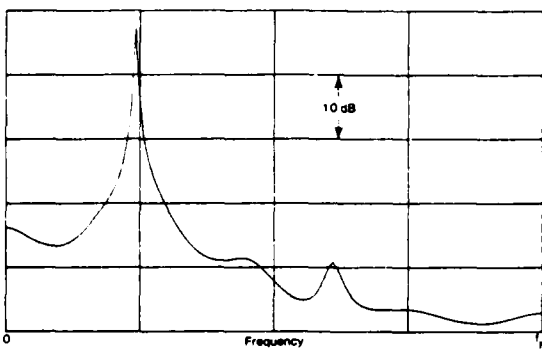


4C. Magnitude-Squared Coherence

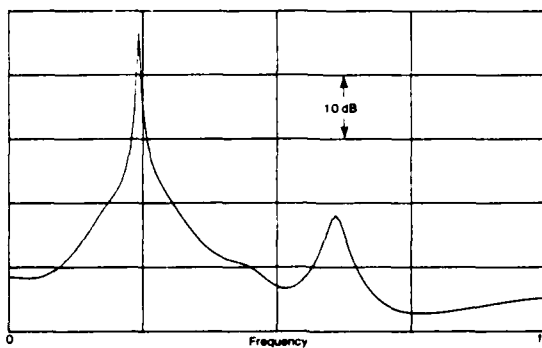


4D. Argument of Complex Coherence

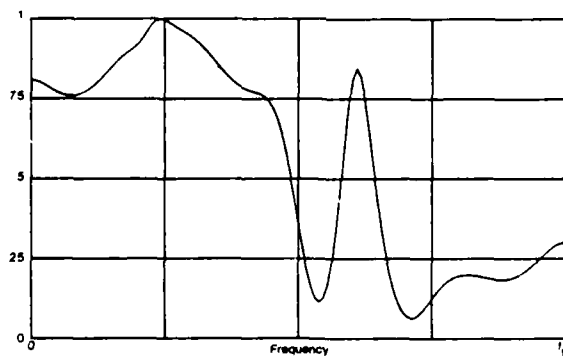
Figure 4. Spectral Estimates for $N = 100$, $P_{max} = 15$, $P_{best} = 4$, Tone Power = -26.9 dB



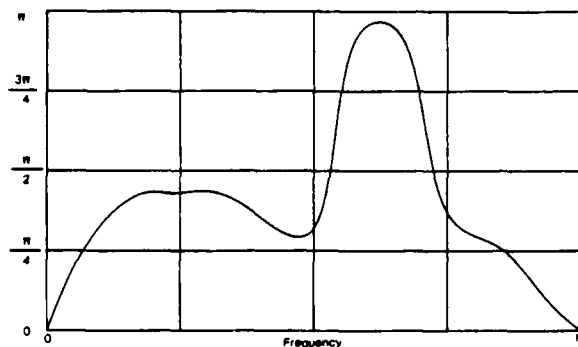
5A. Auto Spectrum of First Process



5B. Auto Spectrum of Second Process



5C. Magnitude-Squared Coherence



5D. Argument of Complex Coherence

Figure 5. Spectral Estimates for $N = 100$, $P_{max} = 15$, $P_{best} = 8$, Tone Power = -20.8 dB

samples of process $\{x_1(k)\}$ alone would not give this tonal indication, since the tone is not present in this process.

The coherence estimates in figure 5 fare no better, even though $P_{best} = 8$ now. A large magnitude-squared coherence value of 0.85 is yielded at frequency $0.6f_N$. The progression towards poorer behavior is also present in figure 6, which employs a tonal power of -14.8 dB relative to the sample power in $\{x_2(k)\}$. Now the undesired peak magnitude-squared coherence estimate is 0.9. A tonal power of -8.8 dB (figure 7) yields a near-unity magnitude-squared coherence estimate at $0.6f_N$, and a very substantial tonal indication in the auto spectrum of $\{x_1(k)\}$, figure 7A.

The situation is markedly improved if more data samples are available. When N is increased to 1000, and data are generated via (5) as before, the sample covariance for the particular data set generated is

$$R_o = \begin{bmatrix} 2.60 & .514 \\ .514 & 2.27 \end{bmatrix} \text{ for } N = 1000, \quad (10)$$

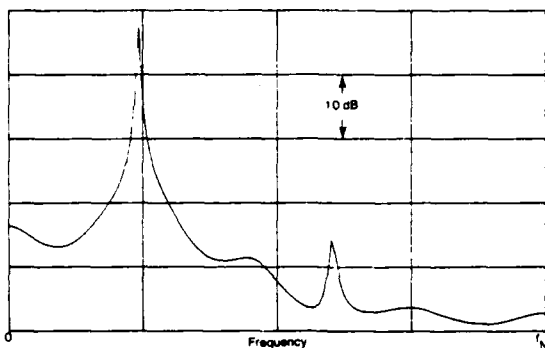
for no tone present. When a tone is added to process $\{x_2(k)\}$, with strength -24.6 dB relative to the sample power, 2.27, of the second process, the resultant spectral estimates are as displayed in figure 8. There is a slight hump at $0.6f_N$ in figure 8B, and a near-zero coherence estimate at this frequency. Recall that the ideal characteristics would be identical to figure 1 except for an impulse in figure 8B at $0.6f_N$ and a very sharp null in the magnitude-squared coherence at $0.6f_N$.

The results in figure 8 were achieved by taking $P_{max} = 8$, for which the AIC indicated $P_{best} = 8$ for this particular data set. However, the AIC is a very flat function of filter order P in this range, and it is difficult to justify a particular value of P as "best". Some additional information about the autoregressive portion of the observed process, such as a limit on P , could be useful; for example, when we specified P_{max} as 1, the results were very similar to figure 1. There was virtually no indication of the tone in any of the spectral estimates, even though it was in the $\{x_2(k)\}$ data at a relative level of -24.6 dB with respect to the sample power, 2.27, of the second autoregressive component. In fact, the estimated first partial correlation coefficient was

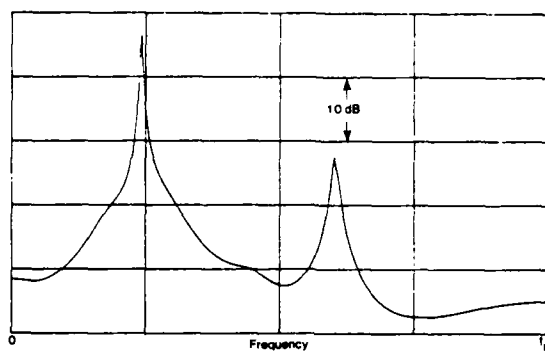
$$A_1^{(1)} = \begin{bmatrix} .8543 & -.7394 \\ .6578 & .5415 \end{bmatrix} \text{ for } N = 1000, \quad (11)$$

which is very close to the true value, (6).

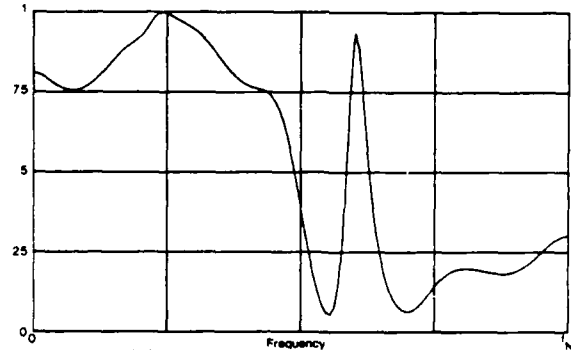
Results for the spectral estimates when the tonal power is increased to -18.6 dB, -12.6 dB, -6.6 dB, and -0.6 dB are given in figures 9, 10, 11, and 12, respectively, all corresponding to $P_{max} = 8$ and $P_{best} = 8$. Even for the nearly 0 dB case in figure 12, there is virtually no indication in auto-spectral estimate 12A of the strong tonal in process $\{x_2(k)\}$, figure 12B. The magnitude-squared coherence estimate in figure 12C appears to have developed a couple of zeros and poles near the frequency $f = 0.6f_N$, where the strong tone is located; recall that we have $4P = 32$ poles available in the approximation for $P_{best} = 8$. Typically, it has been observed that a strong tonal present in only one process manifests itself in the



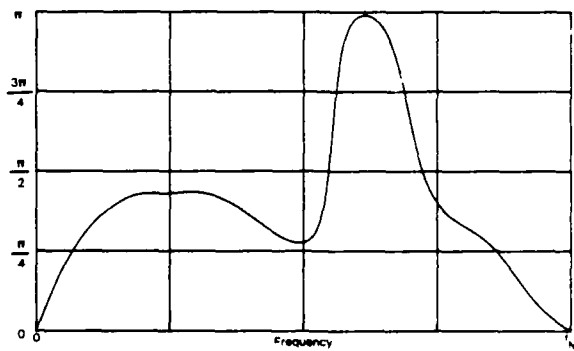
6A. Auto Spectrum of First Process



6B. Auto Spectrum of Second Process

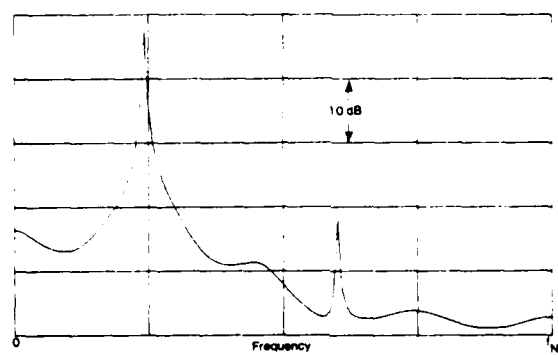


6C. Magnitude-Squared Coherence

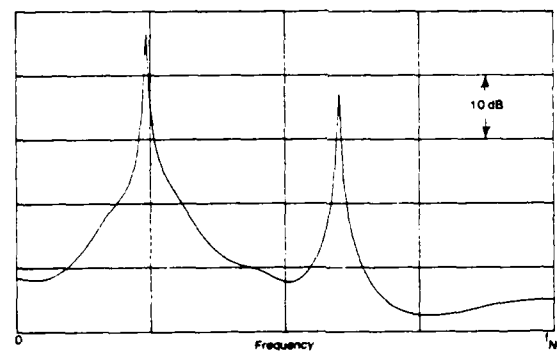


6D. Argument of Complex Coherence

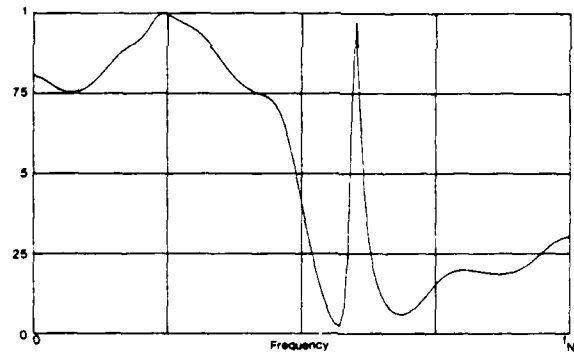
Figure 6. Spectral Estimates for $N = 100$, $P_{max} = 15$, $P_{best} = 8$, Tone Power = -14.8 dB



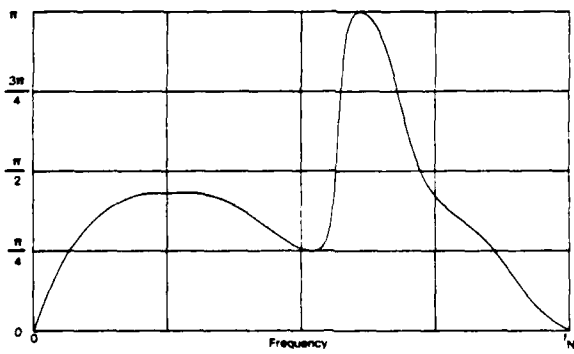
7A. Auto Spectrum of First Process



7B. Auto Spectrum of Second Process

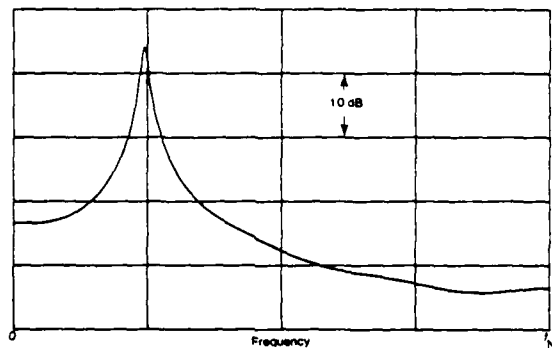


7C. Magnitude-Squared Coherence

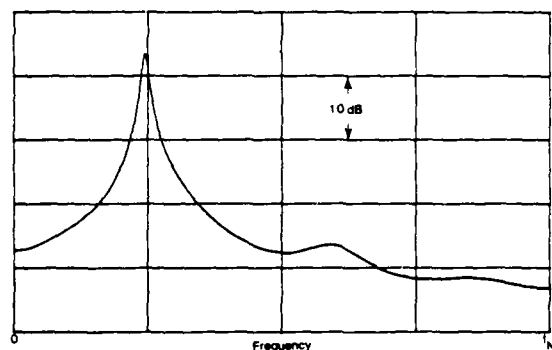


7D. Argument of Complex Coherence

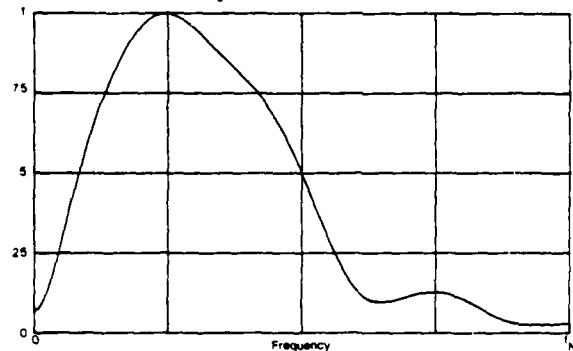
Figure 7. Spectral Estimates for $N = 100$, $P_{max} = 15$, $P_{best} = 8$, Tone Power = -8.8 dB



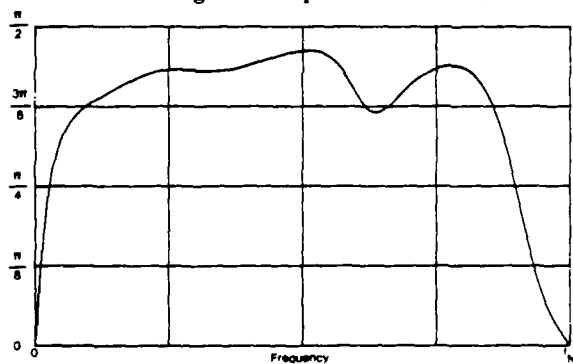
8A. Auto Spectrum of First Process



8B. Auto Spectrum of Second Process



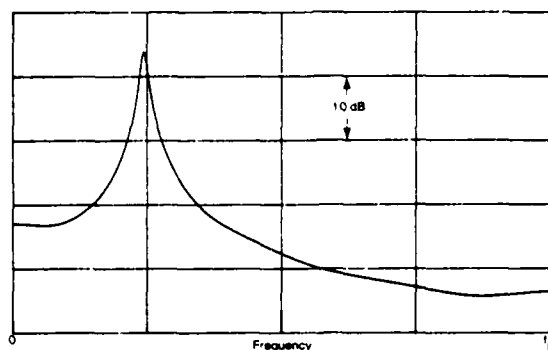
8C. Magnitude-Squared Coherence



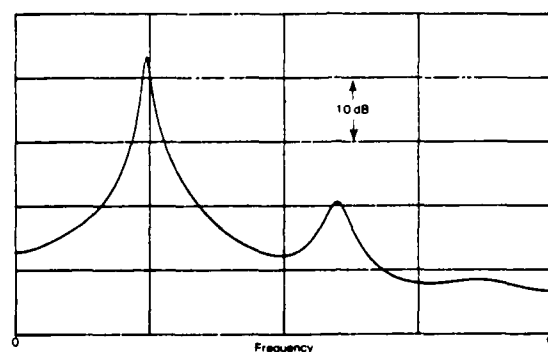
8D. Argument of Complex Coherence

Figure 8. Spectral Estimates for N = 1000, Pmax = 8, Pbest = 8, Tone Power = -24.6 dB

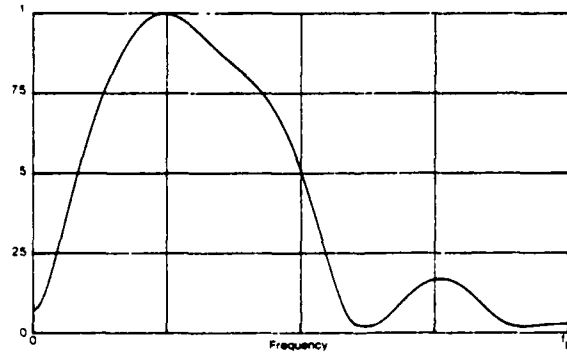
TR 6533



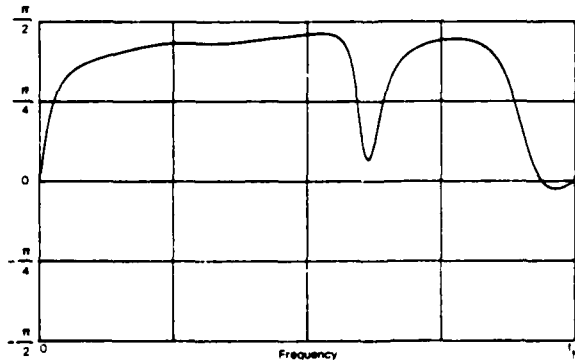
9A. Auto Spectrum of First Process



9B. Auto Spectrum of Second Process

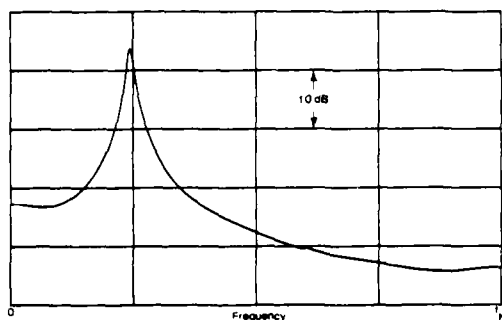


9C. Magnitude-Squared Coherence

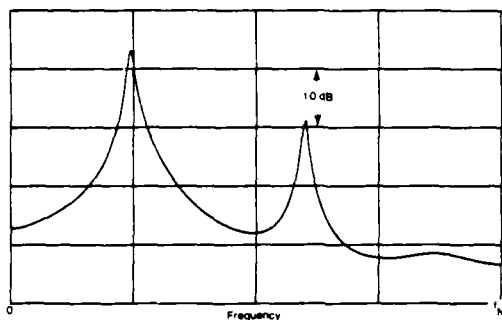


9D. Argument of Complex Coherence

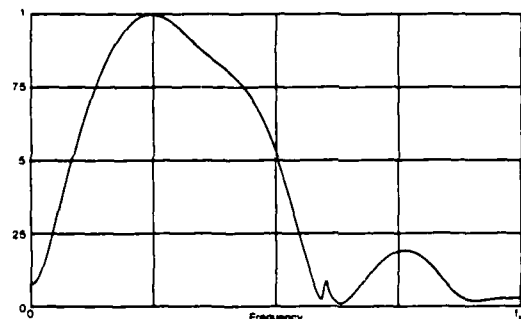
Figure 9. Spectral Estimates for $N = 1000$, $P_{max} = 8$, $P_{best} = 8$, Tone Power = -18.6 dB



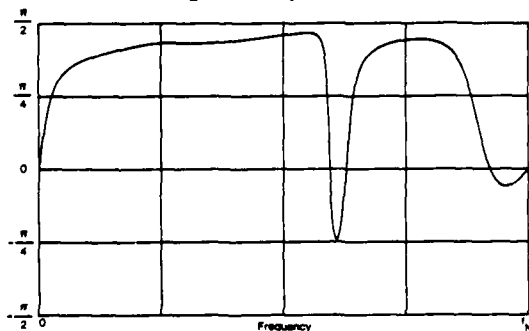
10A. Auto Spectrum of First Process



10B. Auto Spectrum of Second Process

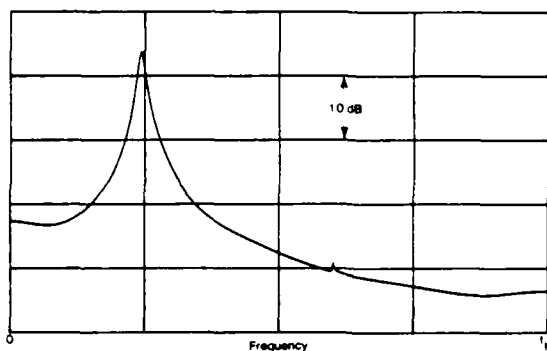


10C. Magnitude-Squared Coherence

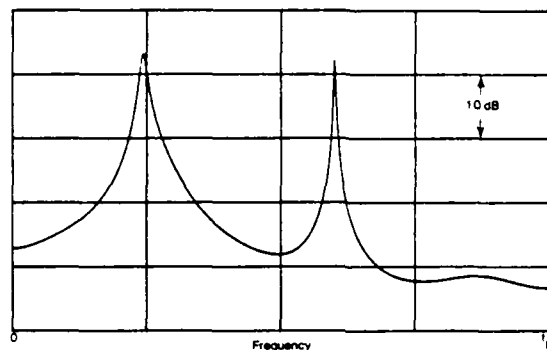


10D. Argument of Complex Coherence

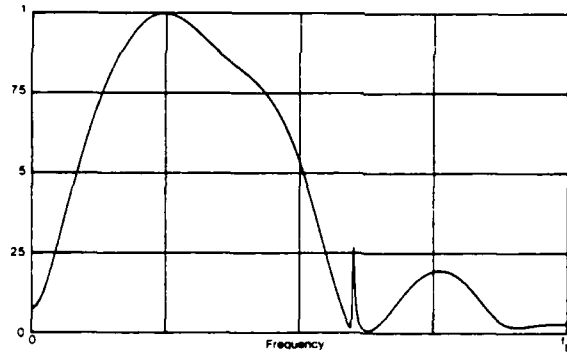
Figure 10. Spectral Estimates for $N = 1000$, $P_{max} = 8$, $P_{best} = 8$, Tone Power = -12.6 dB



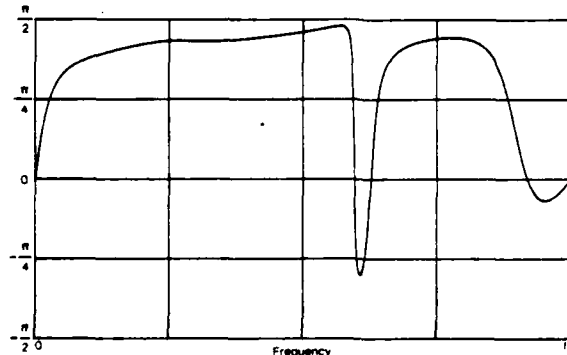
11A. Auto Spectrum of First Process



11B. Auto Spectrum of Second Process

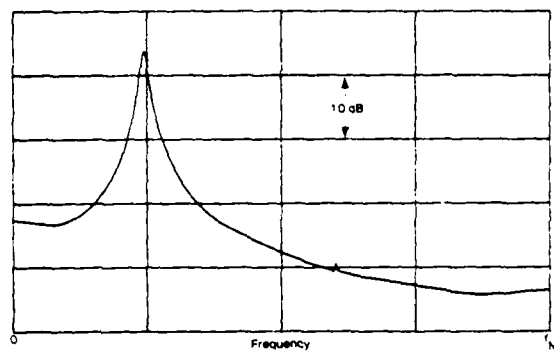


11C. Magnitude-Squared Coherence

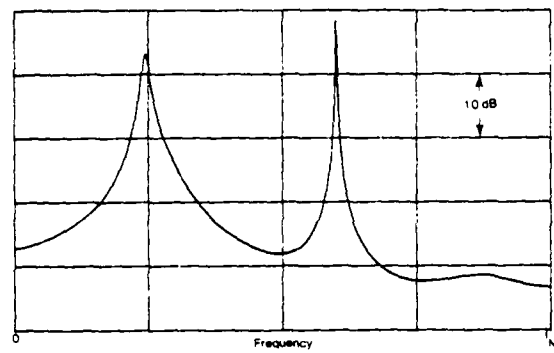


11D. Argument of Complex Coherence

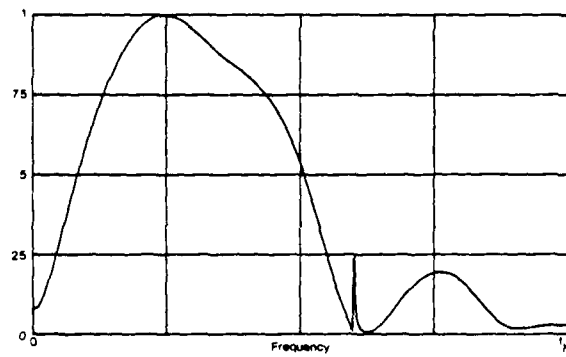
Figure 11. Spectral Estimates for $N = 1000$, $P_{max} = 8$, $P_{best} = 8$, Tone Power = -6.6 dB



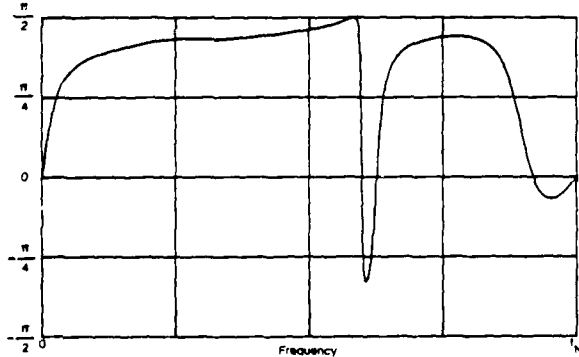
12A. Auto Spectrum of First Process



12B. Auto Spectrum of Second Process



12C. Magnitude-Squared Coherence



12D. Argument of Complex Coherence

Figure 12. Spectral Estimates for $N = 1000$, $P_{max} = 8$, $P_{best} = 8$, Tone Power = -0.6 dB

coherence estimate as a sharp spike at the tone frequency. The change in argument in figure 12D in the neighborhood of this frequency can serve as an indicator of the number of poles and zeros clustered there.

When P_{max} was increased to 47, the AIC yielded $P_{best} = 25$ for these last four figures. However, the spectral estimates for $P_{best} = 25$ proved to be too spiky and erratic. Also the selection of P_{best} at 25 is rather tenuous, as figure 13 indicates; this is a plot of the AIC versus filter order P in the range (1, 47). Although the absolute minimum occurs at $P = 25$, there are significant drops in the curve at $P = 4, 6$, and 8. Selection of P at one of these significant drops appears to be a promising approach, instead of using the absolute minimum of the curve. In addition, the flatness of the curve is brought out by observing that the range of values of AIC is limited to $(-4.80, -4.73)$ for P in the wide range from 10 to 47. Thus, the local minor drops and rises in the AIC curves are not significant; selection of values of P corresponding to significant decreases seems to be a viable approach.

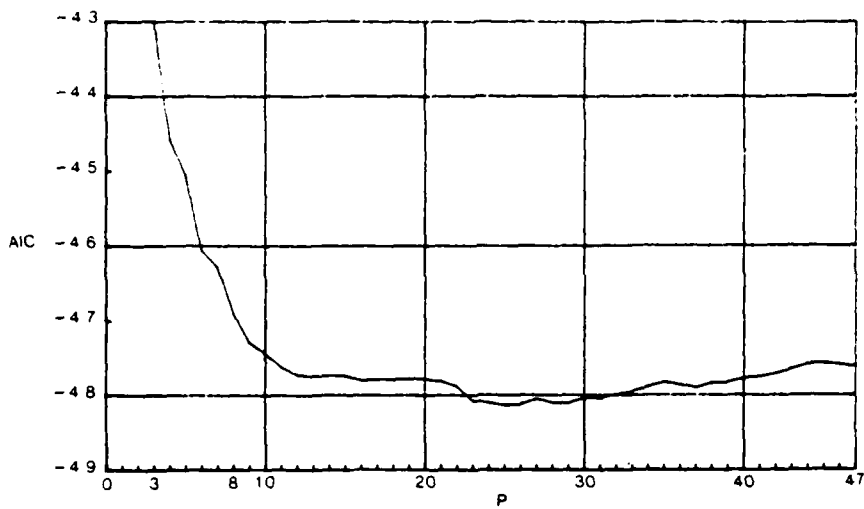
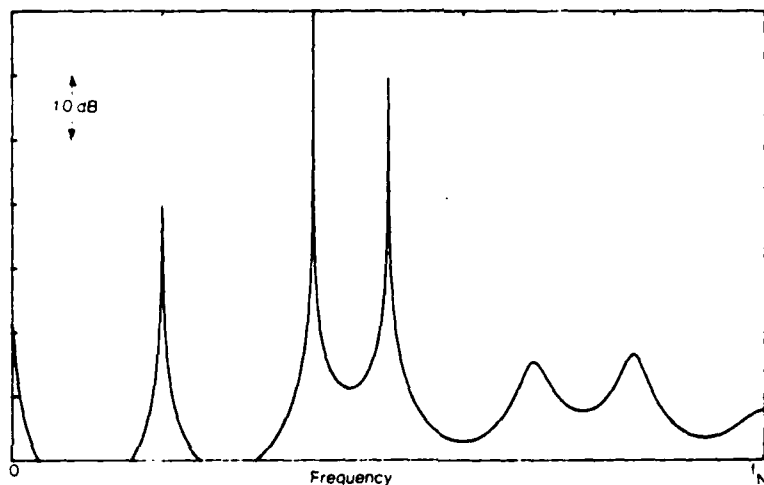


Figure 13. Akaike Information Criterion for $N = 1000$, Tone Power = -12.6 dB

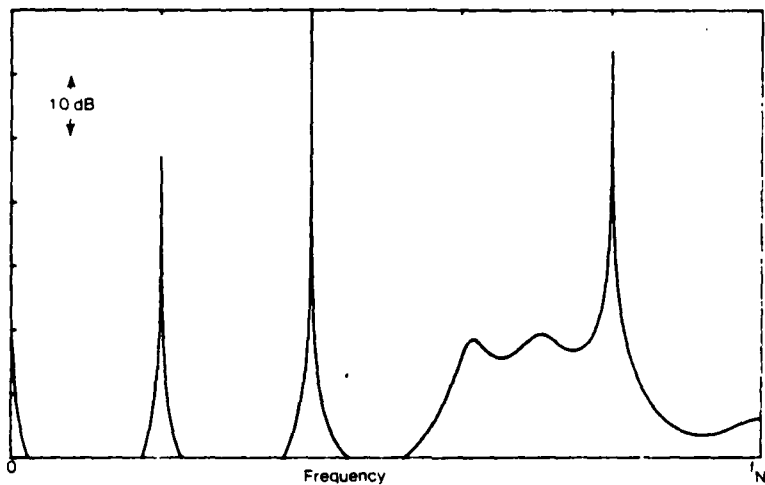
The last example we consider is a two-channel process of $N = 64$ data points, composed of several tones, some of which are at common frequencies, and some of which are not; this example was supplied by S. L. Marple (reference 10). In particular, process $\{x_1(k)\}$ has two strong tones at $f = 0.4f_N$ and $0.5f_N$, and a weaker tone (-20 dB) at $f = 0.2f_N$, in addition to some low level, colored background noise. The other process has two strong tones at $f = 0.4f_N$ and $0.8f_N$, and a weaker tone (-20 dB) at $f = 0.2f_N$. Thus the tonal frequencies common to both processes are $0.2f_N$ and $0.4f_N$, whereas the uncommon frequencies are $0.5f_N$ and $0.8f_N$. The two auto-spectral estimates of each process (obtained via the single-channel, forward-backward averaging technique of reference 4) are displayed in figure 14 for prediction length $P = 12$ (24 poles for each spectral estimate). There is, of course, no cross-feed at frequencies $0.5f_N$ and $0.8f_N$.

The spectral estimates of the same two-channel data (obtained via the program in appendix A which includes coherence estimation) are given in figure 15. The value

of P used was 6, which allows for 24 poles in each spectral estimate. The low number of data points, $N = 64$, now allows some undesired cross-feed in figures 15A and 15B at $f = 0.8f_N$ and $0.5f_N$, respectively. This also shows up in the magnitude-squared coherence estimate as two very sharp spikes at these two frequencies, whereas the true coherence is zero at these two frequencies. This limited capability of the multi-channel linear predictive technique can be improved by utilizing larger data sets; $N = 64$ is too small a data size to accomplish a high quality result for a data set such as this with strong interfering tones.

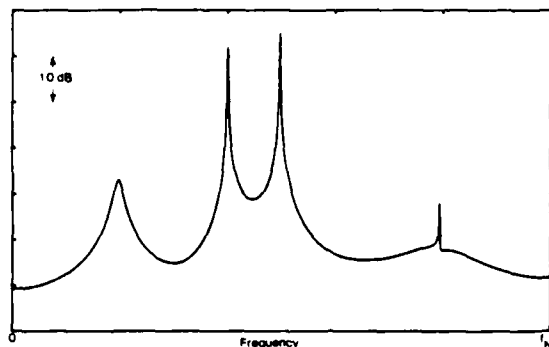


14A. Auto Spectrum of First Process

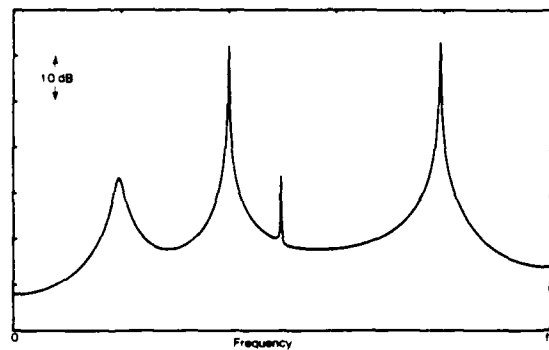


14B. Auto Spectrum of Second Process

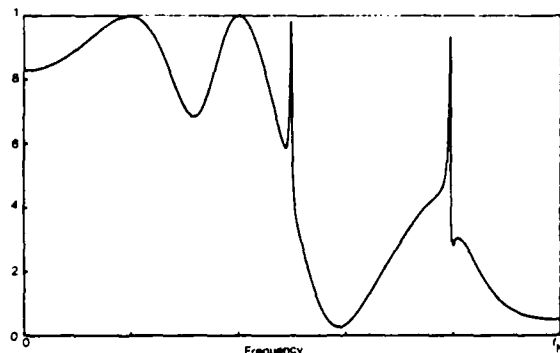
Figure 14. Auto-Spectral Estimates for Multitone Example, $N = 64$, $P = 12$



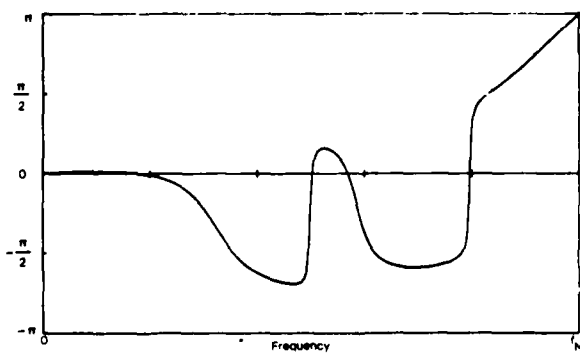
15A. Auto Spectrum of First Process



15B. Auto Spectrum of Second Process



15C. Magnitude-Squared Coherence



15D. Argument of Complex Coherence

Figure 15. Spectral Estimates for Multitone Example, $N = 64$, $P = 6$

Discussion and Conclusions

A program for two-channel auto- and cross-spectral estimation has been presented and illustrated for cases including interfering tones. If the number of available points, N , is too small, some misleading estimates may be obtained because of cross-feed between the finite lengths of data from each channel. This cross-feed manifests itself as narrow spurious spikes in the spectral and coherence estimates. Choice of the appropriate value of filter order, P , is possible by observing where the AIC undergoes significant negative jumps, rather than by using the absolute minimum of the curve. It can also be illuminating to overlay plots made with two (or more) different values of P , thereby obtaining different degrees of resolution and stability from the same data set. The recursive nature of the linear-predictive approach makes this practice easy to achieve.

A more fundamental observation about spectral estimation in general is now developed. Suppose we are given finite data records of three stationary processes $x(t)$, $y(t)$, and $z(t)$, and we wish to estimate all the auto spectra and cross spectra involved. The Blackman and Tukey and weighted-FFT approaches evaluate the auto spectrum of each process separately. Thus, the spectrum of $x(t)$ is estimated without interference from $y(t)$ and $z(t)$; the availability of the data records for $y(t)$ and $z(t)$ plays no part in the eventual auto-spectral estimate for $x(t)$. Additionally, the cross-spectral estimate for processes $x(t)$ and $y(t)$ is independent of the available data on the $z(t)$ process. Finally, the coherence estimate between two processes is independent of any additional data records for other (statistically related) processes.

On the other hand, the generalization (in references 7-9) of Burg's single-channel linear-predictive spectral analysis approach to the multichannel case gives auto-spectral estimates of the $x(t)$ process that are dependent on the available values of $y(t)$ and $z(t)$. Also, the cross-spectral estimate between $x(t)$ and $y(t)$ is dependent on the particular $z(t)$ data available. This procedure can be poor for short data lengths if, for example, $y(t)$ contains a strong tone at f_o that is not present in $x(t)$ or $z(t)$. Thus, estimates of spectra $G_{xx}(f)$, $G_{xy}(f)$, and $G_{xz}(f)$ all contain tonal indications at f_o that should not be there. These spurious tonal indications are due to cross-feed between the available finite data segments of the various processes.

This raises the following questions:

- Should the estimate of $G_{xx}(f)$ be determined only from the available $x(t)$ data record ?
- Should the estimate of $G_{xy}(f)$ be determined only from the available $x(t)$ and $y(t)$ data records ?
- If coherence $C_{xy}(f_o) = 0$, why use $y(t)$ to estimate $G_{xx}(f_o)$?
- If coherence $C_{xy}(f_o) = 1$, why use the completely statistically dependent $y(t)$ data to estimate $G_{xx}(f_o)$?

This philosophy of discarding "irrelevant" data would be consistent with the Blackman and Tukey and FFT approaches. Carrying this philosophy on, we are led to the following: estimate $G_{xx}(f)$ solely from the $x(t)$ data by some good single-

channel linear-predictive technique, such as forward-and-backward averaging, coupled with an efficient way of inverting the relevant matrices (e.g., references 4 and 5). Then estimate cross spectrum $G_{xy}(f)$ or coherence $C(f)$ directly, by some (yet unknown) linear predictive technique whose sole goal is linear prediction of $x(t)$ from $y(t)$ and vice versa, with no interest in or diversion from simultaneous estimation of $G_{xx}(f)$ or $G_{yy}(f)$. By this means, we can concentrate on extracting all the relevant cross-spectral information with maximum stability and resolution. Other cross spectra of interest between particular pairs of available processes can be similarly obtained, one at a time. This procedure is currently under investigation.

Appendix A

Program For Two-Channel Linear-Predictive Spectral Analysis

The program listing below in Basic for the HP 9845B Desk Calculator is a translation and update of that given in references 7-9. A complete breakdown and explanation of the components and subroutines of the program are given in reference 8, and in reference 9, appendix D.

Inputs required of the user are the integers listed in lines 20, 30, 40; they are

N	Number of data points in each process;
Pmax	Maximum order of predictive filter to be considered;
Nfft	Size of FFT to be used in spectral analysis.

In addition, the user must modify subroutine SUB Data(N,X(*)) in lines 5430-5490 at the end of the program to read in his own particular two-channel data sets. Pbest can be forced to equal Pmax by setting Fac = 0 in SUB Pcc.

An explanation of the program output is given under equation (1) of the main text of this report. A sample printout for a short ($N = 20$) data sequence that can be used as a check case on the program is presented following the listing below. Sample plots of the auto-spectral estimates and the coherence estimates conclude the appendix.

```

10 ! TWO-CHANNEL LINEAR PREDICTIVE SPECTRAL ANALYSIS, TR 5501 . 5729
20 N=20           ! NUMBER OF DATA POINTS IN EACH PROCESS
30 Pmax=6         ! MAXIMUM ORDER OF PREDICTIVE FILTER
40 Nfft=256       ! SIZE OF FFT
50 OPTION BASE 1
60 REDIM Y(2,N),Z(2,N),Ap(Pmax,2,2),Bp(Pmax,2,2)
70 REDIM Rn(Pmax,2,2),Aic(0:Pmax),X11(Nfft),Y11(Nfft),X12(Nfft)
80 REDIM Y12(Nfft),X21(Nfft),Y21(Nfft),X22(Nfft),Y22(Nfft)
90 DIM Y(2,1000),Z(2,1000),Ap(25,2,2),Bp(25,2,2)
100 DIM Rn(25,2,2),Aic(0:25),X11(1024),Y11(1024),X12(1024)
110 DIM Y12(1024),X21(1024),Y21(1024),X22(1024)
120 DIM Ave(2,2),Ubest(2,2),U(2,2),V(2,2),Ui(2,2),Vi(2,2),R(2,2)
130 DIM B(2,2),R(2,2),Wa(2,2),Wb(2,2),Wc(2,2),Wd(2,2),We(2,2)
140 PRINT "NUMBER OF DATA POINTS IN EACH PROCESS N =";N
150 PRINT "MAXIMUM ORDER OF PREDICTIVE FILTER Pmax =";Pmax
160 PRINT "SIZE OF FFT Nfft =";Nfft
170 PRINT
180 CALL Data(N,Y(*))
190 PRINT "PROCESS NUMBER 1"
200 FOR I=1 TO N
210 PRINT Y(1,I);
220 NEXT I
230 PRINT LIN(1)
240 PRINT "PROCESS NUMBER 2"
250 FOR I=1 TO N
260 PRINT Y(2,I);
270 NEXT I
280 PRINT LIN(2)
290 CALL Pcc(N,Pmax,Y(*),Z(*),Rn(*),Wa(*),Wb(*),Wc(*),Wd(*),We(*),Ri(*),Ui(*),Vi(*),
      Aic(*),Pbest,Ubest(*),Ui(*),Vi(*),Ri(*),Bi(*),Ap(*),Bp(*))
300 PRINT "MEANS OF INPUT DATA (Ave)"
310 PRINT Ave(1)
320 PRINT Ave(2)
330 PRINT LIN(1)
340 PRINT "COVARIANCE MATRIX OF INPUT DATA (R):",R(*)
350 PRINT "AKAIKE INFORMATION CRITERION:"
360 PRINT " P          Aic(P)"
370 IMAGE 3D,4(4X,M, 9DE)
380 FOR P=0 TO Pmax
390 PPINT USING 370;P,Aic(P)
400 NEXT P
410 PRINT LIN(1)
420 PRINT "Pbest =";Pbest
430 PRINT LIN(1)
440 PRINT "Ubest:",Ubest(*)
450 PRINT "FORWARD PARTIAL CORRELATION COEFFICIENTS:"
460 PRINT " P          Ap(1,1)          Ap(2,1)          Ap(1,2)
      Ap(2,2)"
470 FOR P=1 TO Pmax
480 PRINT USING 370;P,Ap(P,1,1),Ap(P,2,1),Ap(P,1,2),Ap(P,2,2)
490 NEXT P
500 PRINT LIN(1)

```

```

510 PRINT "BACKWARD PARTIAL CORRELATION COEFFICIENTS:"
520 PRINT " P Bp(1,1) Bp(2,1) Bp(1,2)
      Bp(2,2)"
530 FOR P=1 TO Pmax
540 PRINT USING 370;P,Bp(P,1,1),Bp(P,2,1),Bp(P,1,2),Bp(P,2,2)
550 NEXT P
560 PRINT LIN(1)
570 IF Pbest=0 THEN 890
580 CALL Pfc(Pmax,Pbest,R(*),Rp(*),Bp(*),Wa(*),Wb(*),Wc(*),Rn(*),R11,R22
      ,R12)
590 PRINT "FORWARD PREDICTIVE FILTER COEFFICIENTS FOR Pbest:"
600 PRINT " P Rp(1,1) Rp(2,1) Rp(1,2)
      Rp(2,2)"
610 FOR P=1 TO Pbest
620 PRINT USING 370;P,Rp(P,1,1),Rp(P,2,1),Rp(P,1,2),Rp(P,2,2)
630 NEXT P
640 PRINT LIN(1)
650 PRINT "NORMALIZED CORRELATION MATRICES (Rn):"
660 PRINT "DELAY AUTO11 CROSS12
      AUTO22"
670 PRINT USING 370;0,R(1,1),R(2,1),R(1,2),R(2,2)
680 FOR P=1 TO Pmax
690 PRINT USING 370;P,Rn(P,1,1),Rn(P,2,1),Rn(P,1,2),Rn(P,2,2)
700 NEXT P
710 PRINT LIN(1)
720 CALL Peftf(Pbest,Nfft,Ap(*),X11(*),Y11(*),X12(*),Y12(*),X21(*),Y21(*),X22
      (*),Y22(*))
730 CALL Sdm(Nfft,Ubest(*),Wa(*),Wb(*),Wc(*),Wd(*),We(*),X11(*),Y11(*),X12(*),
      Y12(*),X21(*),Y21(*),X22(*),Y22(*),S11,S22,S12)
740 PRINT "SPECTRAL DENSITY MATRIX AND COHERENCE, FROM ZERO FREQUENCY - BIN 1/:
      "
750 PRINT " BIN AUTO11 AUTO22 RE(CROSS12) IM(CROSS12) MAG SQ COH
      ARGUMENT"
760 IMAGE 3D,5(M.6DE,1X),M.6DE
770 FOR I=1 TO 30
780 L=I
790 IF I<16 THEN 840
800 IF I>16 THEN 830
810 PRINT "***"
820 GOTO 850
830 L=I+Nfft/2-29
840 PRINT USING 760;L,X11(L),X22(L),X12(L),Y12(L),Y11(L),Y22(L)
850 NEXT I
860 PRINT LIN(1)
870 PRINT "TRAPEZOIDAL SUMS OF SPECTRA:"
880 PRINT S11,S22,S12
890 PRINT
900 PRINT "COVARIANCES OF INPUT DATA:"
910 PRINT R11,R22,R12
920 PRINT LIN(1)
930 CALL Rcm(Nfft,X11(*),X12(*),Y12(*),X21(*),Y21(*),X22(*),X11m1,X22m1,X11m0,
      X22m0)
940 N1=Nfft+1
950 N2=Nfft/2
960 N22=N2+2

```

TR 6533

```
970 PRINT "ALIASED NORMALIZED CORRELATION MATRICES:"  
980 PRINT "DELAY AUTO11 CROSS21 CROSSE12  
AUTO22"  
990 PRINT USING 370;0,X11(N22),X21(1),..,X21(1),X22(N22)  
1000 FOR I=1 TO 27  
1010 L=I  
1020 IF I > 16 THEN 1070  
1030 IF I < 16 THEN 1060  
1040 PRINT "****"  
1050 GOTO 1080  
1060 L=I+N2-29  
1070 PRINT USING 370;L,X11(N22+L),X21(N1-L),X21(1+L),X22(N2+L)  
1080 NEXT I  
1090 PRINT USING 370;N2-1,X11m1,X21(N22),X21(N2),X22m1  
1100 PRINT USING 370;N2,X11m0,X21(N2+1),X21(N2+1),X22m0  
1110 PRINT LIN(2)  
1120 PRINTER IS 0  
1130 PRINT "AUTO SPECTRAL DENSITIES IN DB:"  
1140 PLOTTER IS "GRAPHICS"  
1150 GRAPHICS  
1160 SCALE 0,N2,-5,0  
1170 GRID N2/4,1  
1180 PENUP  
1190 FOR I=0 TO N2  
1200 PLOT I,LGT(X11(I+1))  
1210 NEXT I  
1220 PENUP  
1230 FOR I=0 TO N2  
1240 PLOT I,LGT(X22(I+1))  
1250 NEXT I  
1260 PENUP  
1270 DUMP GRAPHICS  
1280 PRINT LIN(3)  
1290 PRINT "MAGNITUDE SQUARED COHERENCE AND ARGUMENT"  
1300 PLOTTER IS "GRAPHICS"  
1310 SCALE 0,N2,0,1  
1320 GRID N2/4,.25  
1330 PENUP  
1340 FOR I=0 TO N2  
1350 PLOT I,Y11(I+1)  
1360 NEXT I  
1370 PENUP  
1380 SCALE 0,N2,-PI,PI  
1390 FOR I=0 TO N2  
1400 PLOT I,Y22(I+1)  
1410 NEXT I  
1420 PENUP  
1430 DUMP GRAPHICS  
1440 PRINT LIN(4)  
1450 PRINTER IS 16  
1460 END  
1470 !
```

```

1480 SUB Fcc(N,Pmax,Y(*),Z(*),Avec(*),Wav(*),WB(*),WD(*),WC(*),U(*),
* ,Aic(*),Pbest,Ubest(*),U1(*),V1(*),A1(*),B1(*),Rp(*),Bp(*),Bpm(*)
1490 Ia=INT(1.5+SQR(N))
1500 IF Pmax>=Ia THEN 1520
1510 PRINT "Pmax =";Pmax;" IS TOO LARGE FOR N =";N;" SEARCH LIMITED TO P =";Ia
1520 Ia=MIN(Ia,Pmax)
1530 Fac=8*N ! Fac=0 WOULD FORCE Pbest EQUAL TO Pma
1540 MAT Ave=RSUM(Y)
1550 MAT Ave=Ave/N
1560 A1=Ave(1)
1570 A2=Ave(2)
1580 FOR I=1 TO N
1590 Y(1,I)=Y(1,I)-A1
1600 Y(2,I)=Y(2,I)-A2
1610 NEXT I
1620 MAT Z=Y
1630 CALL Auto(2,N-1,Y(*),Wc(*))
1640 CALL Auto(1,1,Y(*),Wd(*))
1650 CALL Auto(N,N,Y(*),We(*))
1660 MAT Wa=Wc+We
1670 MAT Wb=Wc+Wd
1680 MAT R=Wb+We
1690 MAT R=R/(N)
1700 MAT U=R
1710 MAT V=R
1720 CALL Cross(2,N,Y(*),Z(*),Wc(*))
1730 Aic(0)=LOG(DET(U))
1740 Aicmin=Aic(0)
1750 Pbest=0
1760 MAT Ubest=U
1770 FOR P=1 TO Ia
1780 MAT Vi=INV(V)
1790 MAT Wd=Vi*Wb
1800 MAT Wb=Wd
1810 MATUi=INV(U)
1820 MAT Wd=Wa
1830 MAT Wa=Wd*Ui
1840 MAT Wc=Wc*(2)
1850 CALL Solve(Wa(*),Wb(*),Wc(*),Wd(*),We(*))
1860 MAT A=Wc*Vi
1870 MAT Wd=TRN(Wc)
1880 MAT B=Wd*Ui
1890 Ap(P,1,1)=A(1,1)
1900 Ap(P,1,2)=A(1,2)
1910 Ap(P,2,1)=A(2,1)
1920 Ap(P,2,2)=A(2,2)
1930 Bp(P,1,1)=B(1,1)
1940 Bp(P,1,2)=B(1,2)
1950 Bp(P,2,1)=B(2,1)
1960 Bp(P,2,2)=B(2,2)
1970 MAT We=A*Wd
1980 MAT U=U-We
1990 MAT We=B*Wc
2000 MAT V=V-We

```

```

2010 Ric(P)=LOG(DET(U))+Fac*P
2020 IF Ric(P)>=Ricmin THEN 2060
2030 Ricmin=Ric(P)
2040 Pbest=P
2050 MAT Ubest=U
2060 IF P=Ia THEN 2220
2070 L=P+1
2080 FOR K=N TO L STEP -1
2090 A1=Y(1,K)
2100 A2=Y(2,K)
2110 B1=Z(1,K-1)
2120 B2=Z(2,K-1)
2130 Z(1,K)=B1-B(1,1)*A1-B(1,2)*A2
2140 Z(2,K)=B2-B(2,1)*A1-B(2,2)*A2
2150 Y(1,K)=A1-A(1,1)*B1-A(1,2)*B2
2160 Y(2,K)=A2-A(2,1)*B1-A(2,2)*B2
2170 NEXT K
2180 CALL Auto(P+2,N,Y(*),Wa(*))
2190 CALL Auto(P+1,N-1,Z(*),Wb(*))
2200 CALL Cross(P+2,N,Y(*),Z(*),Wc(*))
2210 NEXT P
2220 A1=.5*(Ubest(1,2)+Ubest(2,1))
2230 Ubest(1,2)=Ubest(2,1)=A1
2240 SUBEND
2250 !
2260 SUB Ffc(Pmax,Pbest,R(*),Rp(*),Bp(*),Wa(*),Wb(*),Wc(*),Rn(*),R11,F22,
R12)
2270 Rn(1,1,1)=Rp(1,1,1)*R(1,1,1)+Rp(1,1,2)*R(2,1,1)
2280 Rn(1,1,2)=Rp(1,1,1)*R(1,2,1)+Rp(1,1,2)*R(2,2,1)
2290 Rn(1,2,1)=Rp(1,2,1)*R(1,1,1)+Rp(1,2,2)*R(2,1,1)
2300 Rn(1,2,2)=Rp(1,2,1)*R(1,2,1)+Rp(1,2,2)*R(2,2,1)
2310 FOR P=2 TO Pbest
2320 Wc(1,1)=Rp(P,1,1)*R(1,1,1)+Rp(P,1,2)*R(2,1,1)
2330 Wc(1,2)=Rp(P,1,1)*R(1,2,1)+Rp(P,1,2)*R(2,2,1)
2340 Wc(2,1)=Rp(P,2,1)*R(1,1,1)+Rp(P,2,2)*R(2,1,1)
2350 Wc(2,2)=Rp(P,2,1)*R(1,2,1)+Rp(P,2,2)*R(2,2,1)
2360 FOR L=1 TO P-1
2370 Ib=P-L
2380 Wa(1,1)=Rp(P,1,1)*Bp(Ib,1,1)+Rp(P,1,2)*Bp(Ib,2,1)
2390 Wa(1,2)=Rp(P,1,1)*Bp(Ib,1,2)+Rp(P,1,2)*Bp(Ib,2,2)
2400 Wa(2,1)=Rp(P,2,1)*Bp(Ib,1,1)+Rp(P,2,2)*Bp(Ib,2,1)
2410 Wa(2,2)=Rp(P,2,1)*Bp(Ib,1,2)+Rp(P,2,2)*Bp(Ib,2,2)
2420 Wa(1,1)=Rp(L,1,1)-Wa(1,1)
2430 Wa(1,2)=Rp(L,1,2)-Wa(1,2)
2440 Wa(2,1)=Rp(L,2,1)-Wa(2,1)
2450 Wa(2,2)=Rp(L,2,2)-Wa(2,2)

```

```

2460 Wb(1,1)=Bp(P,1,1)*Rp(L,1,1)+Bp(F,1,2)*Rp(L,2,1)
2470 Wb(1,2)=Bp(P,1,1)*Rp(L,1,2)+Bp(F,1,2)*Rp(L,2,2)
2480 Wb(2,1)=Bp(P,2,1)*Rp(L,1,1)+Bp(P,2,2)*Rp(L,2,1)
2490 Wb(2,2)=Bp(P,2,1)*Rp(L,1,2)+Bp(P,2,2)*Rp(L,2,2)
2500 Bp(Ib,1,1)=Bp(Ib,1,1)-Wb(1,1)
2510 Bp(Ib,1,2)=Bp(Ib,1,2)-Wb(1,2)
2520 Bp(Ib,2,1)=Bp(Ib,2,1)-Wb(2,1)
2530 Bp(Ib,2,2)=Bp(Ib,2,2)-Wb(2,2)
2540 Rp(L,1,1)=Wa(1,1)
2550 Rp(L,1,2)=Wa(1,2)
2560 Rp(L,2,1)=Wa(2,1)
2570 Rp(L,2,2)=Wa(2,2)
2580 Wd(1,1)=Wa(1,1)*Rn(Ib,1,1)+Wa(1,2)*Rn(Ib,2,1)
2590 Wd(1,2)=Wa(1,1)*Rn(Ib,1,2)+Wa(1,2)*Rn(Ib,2,2)
2600 Wd(2,1)=Wa(2,1)*Rn(Ib,1,1)+Wa(2,2)*Rn(Ib,2,1)
2610 Wd(2,2)=Wa(2,1)*Rn(Ib,1,2)+Wa(2,2)*Rn(Ib,2,2)
2620 MAT Wc=Wc+Wd
2630 NEXT L
2640 Rn(P,1,1)=Wc(1,1)
2650 Rn(P,1,2)=Wc(1,2)
2660 Rn(P,2,1)=Wc(2,1)
2670 Rn(P,2,2)=Wc(2,2)
2680 NEXT P
2690 FOR P=Pbest+1 TO Pmax
2700 MAT Wa=ZER
2710 FOR L=1 TO Pb
2720 Ib=P-L
2730 Wb(1,1)=Rp(L,1,1)*Rn(Ib,1,1)+Rp(L,1,2)*Rn(Ib,2,1)
2740 Wb(1,2)=Rp(L,1,1)*Rn(Ib,1,2)+Rp(L,1,2)*Rn(Ib,2,2)
2750 Wb(2,1)=Rp(L,2,1)*Rn(Ib,1,1)+Rp(L,2,2)*Rn(Ib,2,1)
2760 Wb(2,2)=Rp(L,2,1)*Rn(Ib,1,2)+Rp(L,2,2)*Rn(Ib,2,2)
2770 MAT Wa=Wa+Wb
2780 NEXT L
2790 Rn(P,1,1)=Wa(1,1)
2800 Rn(P,1,2)=Wa(1,2)
2810 Rn(P,2,1)=Wa(2,1)
2820 Rn(P,2,2)=Wa(2,2)
2830 NEXT P
2840 R11=R(1,1)
2850 R22=R(2,2)
2860 R12=R(1,2)
2870 T=SQR(R11*R22)
2880 R(1,1)=R(2,2)=1
2890 R(1,2)=R(2,1)=R12/T
2900 FOR P=1 TO Pmax
2910 Rn(P,1,1)=Rn(P,1,1)/R11
2920 Rn(P,1,2)=Rn(P,1,2)/T
2930 Rn(P,2,1)=Rn(P,2,1)/T
2940 Rn(P,2,2)=Rn(P,2,2)/R22
2950 NEXT P
2960 SUBEND
2970 !

```

TR 6533

```

2960 SUB Pfft1·Pbest,Nfft,Ap(++,X11(++)·X11(+-),X2(+-),X12(+-),X21(+-),X21(+-),X22(+-)
1,X22(+-))
2990 X11(1)=X22(1)=1
3000 FOR L=1 TO Pbest
3010 X11(L+1)=-Ap(L,1,1)
3020 X12(L+1)=-Ap(L,1,2)
3030 X21(L+1)=-Ap(L,2,1)
3040 X22(L+1)=-Ap(L,2,2)
3050 NEXT L
3060 CALL Fft10(Nfft,X11(*),Y11(*))
3070 CALL Fft10(Nfft,X12(*),Y12(*))
3080 CALL Fft10(Nfft,X21(*),Y21(*))
3090 CALL Fft10(Nfft,X22(*),Y22(*))
3100 SUBEND
3110 !
3120 SUB Sdm·Nfft,Ubest(+),Wa(+),Wb(+),Wc(+),Wd(+),We(+),S11(+),Y11(+),X12(+),Y12(+),
1,X21(+),Y21(+),X22(+),Y22(+),S11,S22,S12
3130 T=2 Nfft
3140 S11=S22=S12=0
3150 J=Nfft-2+1
3160 FOR L=1 TO J
3170 Wa(1,1)=X22(L)
3180 Wa(1,2)=-X12(L)
3190 Wa(2,1)=-X21(L)
3200 Wa(2,2)=X11(L)
3210 Wb(1,1)=Y22(L)
3220 Wb(1,2)=-Y12(L)
3230 Wb(2,1)=-Y21(L)
3240 Wb(2,2)=Y11(L)
3250 Ta=DET(Wa)-DET(Wb)
3260 Tb=Wa(1,1)*Wb(2,2)+Wa(2,2)*Wb(1,1)-Wa(1,2)*Wb(2,1)-Wa(2,1)*Wb(1,2)
3270 Ta=T/(Ta*Tb)
3280 MAT Wc=TRN(Wa)
3290 MAT Wd=Ubest*Wc
3300 MAT Wc=Wb*Wd
3310 Tb=Wc(1,2)-Wc(2,1)
3320 MAT Wc=Wa*Wd
3330 MAT Wd=TRN(Wb)
3340 MAT We=Ubest*Wd
3350 MAT Wd=Wb*We
3360 MAT Wc=Wc+Wd
3370 Y11(L)=(Wc(1,2)^2+Tb*Tb)/(Wc(1,1)*Wc(2,2))
3380 Y22(L)=FNArg(Wc(1,2),Tb)
3390 X11(L)=Ta*Wc(1,1)
3400 X22(L)=Ta*Wc(2,2)
3410 X12(L)=Ta*Wc(1,2)
3420 Y12(L)=Ta*Tb
3430 S11=S11+X11(L)
3440 S22=S22+X22(L)
3450 S12=S12+X12(L)
3460 NEXT L
3470 S11=S11-.5*(X11(1)+X11(J))
3480 S22=S22-.5*(X22(1)+X22(J))
3490 S12=S12-.5*(X12(1)+X12(J))
3500 SUBEND
3510 !

```

```

3520 SUB Rcm(Nfft,X11(*),X12(*),Y12(*),X21(*), X1(*),X2(*),X11m1,X22m1,X11m0,X
22m0)
3530 N2=Nfft-2
3540 N21=N2+1
3550 N22=N2+2
3560 FOR L=1 TO N2
3570 X21(L)=.5*X11(L)
3580 Y21(L)=.5*X22(L)
3590 X21(N2+L)=.5*X11(N22-L)
3600 Y21(N2+L)=.5*X22(N22-L)
3610 NEXT L
3620 CALL Fft10(Nfft,X21(*),Y21(*))
3630 Ta=1/X21(1)
3640 Tb=1/Y21(1)
3650 T=SQR(Ta*Tb)
3660 X11(N22)=X22(N22)=1
3670 FOR L=2 TO N2-1
3680 X11(N21+L)=X21(L)*Ta
3690 X22(N21+L)=Y21(L)*Tb
3700 NEXT L
3710 X11m1=X21(N2)*Ta
3720 X22m1=Y21(N2)*Tb
3730 X11m0=X21(N21)*Ta
3740 X22m0=Y21(N21)*Tb
3750 X21(1)=.5*X12(1)*T
3760 Y21(1)=-.5*Y12(1)*T
3770 FOR L=2 TO N2
3780 X21(L)=X12(L)*T
3790 Y21(L)=-Y12(L)*T
3800 X21(N2+L)=Y21(N2+L)=0
3810 NEXT L
3820 X21(N21)=.5*X12(N21)*T
3830 Y21(N21)=-.5*Y12(N21)*T
3840 CALL Fft10(Nfft,X21(*),Y21(*))
3850 SUBEND
3860 !

```

TR 6533

```
3870 SUB Cross(N1,N2,A(*),B(*),C(*))
3880 S11=S12=S21=S22=0
3890 FOR K=N1 TO N2
3900 A1=A(1,K)
3910 A2=A(2,K)
3920 B1=B(1,K-1)
3930 B2=B(2,K-1)
3940 S11=S11+A1*B1
3950 S12=S12+A1*B2
3960 S21=S21+A2*B1
3970 S22=S22+A2*B2
3980 NEXT K
3990 C(1,1)=S11
4000 C(1,2)=S12
4010 C(2,1)=S21
4020 C(2,2)=S22
4030 SUBEND
4040 !
4050 SUB Auto(N1,N2,A(*),B(*))
4060 S11=S12=S22=0
4070 FOR K=N1 TO N2
4080 A1=A(1,K)
4090 A2=A(2,K)
4100 S11=S11+A1*A1
4110 S12=S12+A1*A2
4120 S22=S22+A2*A2
4130 NEXT K
4140 B(1,1)=S11
4150 B(1,2)=B(2,1)=S12
4160 B(2,2)=S22
4170 SUBEND
4180 !
4190 SUB Solve(Wa(*),Wb(*),Wc(*),Wd(*),We(*))
4200 Ta=Wa(1,1)+Wa(2,2)+Wb(1,1)+Wb(2,2)
4210 Tb=DET(Wa)-DET(Wb)
4220 MAT Wd=Wc*Wb
4230 We(1,1)=Wa(2,2)
4240 We(1,2)=-Wa(1,2)
4250 We(2,1)=-Wa(2,1)
4260 We(2,2)=Wa(1,1)
4270 MAT Wa=We*Wc
4280 MAT Wd=Wd+Wa
4290 MAT Wb=Wb*(Ta)
4300 Wb(1,1)=Wb(1,1)+Tb
4310 Wb(2,2)=Wb(2,2)+Tb
4320 MAT We=INV(Wb)
4330 MAT Wc=Wd*We
4340 SUBEND
4350 !
```

```

4360 SUB Fft10(N,M+,V++)    ! N = 2 10 = 1024, M=2 INTEGER
4370 DIM C(1:257)
4380 DATA 1,.999981175283,.999924701819,.999930511736,.999938818696,.9995294175
01,.999322384588,.999077727753,.998795456205,.998475580573,.998118112900
4390 DATA .997723066644,.997290456679,.996820299191,.996312612182,.995767414468
,.995184726672,.994564570724,.993906870001,.993211843215,.992479534599
4400 DATA .991709753669,.990902635428,.990658102621,.990179509965,.988257567751
,.987301418158,.986308097245,.985277642369,.984210091187,.983105487431
4410 DATA .981963869110,.980785280403,.979568765665,.978317370720,.977026142658
,.975702130039,.974339382786,.972939952206,.971502889996,.970031253195
4420 DATA .968522094274,.966976471045,.965394441698,.963776065795,.962121404269
,.960430519416,.958703474896,.956940335731,.955141168306,.953306040354
4430 DATA .951435020969,.949528180593,.947565591018,.945607325381,.943593458162
,.941544065183,.939459223602,.937339011913,.935183509939,.932992798835
4440 DATA .930766961079,.928506080473,.926210242138,.923879532511,.921514039342
,.919113851630,.916679059921,.914209755704,.911705032005,.909167963091
4450 DATA .906595704515,.903989293123,.901348847048,.898674465694,.895966249756
,.893224301196,.890448723245,.887639620403,.884797096431,.881921264348
4460 DATA .879012226429,.876070094195,.873094376416,.870086991109,.867046245516
,.863372856122,.860866938638,.857728610000,.854557988365,.851355193105
4470 DATA .848120344903,.844853565250,.841554977437,.838224705555,.834862874986
,.831469612303,.828045045258,.824589302785,.821102514391,.817584813152
4480 DATA .814036329706,.810457198253,.806347553544,.803207531481,.799537269108
,.795336904609,.792106577300,.788346427627,.784556597156,.780737228572
4490 DATA .776888465673,.773010453363,.768103337646,.765167265622,.761202385434
,.757208846506,.753186799044,.749136394523,.745057785441,.740951125355
4500 DATA .736816568877,.732654271672,.728464390448,.724247082951,.720002507961
,.715730825284,.711432195745,.707106781187,.702754744457,.698376249409
4510 DATA .693971456890,.689540544737,.685033667773,.680600997795,.676092703575
,.671558954847,.666999922304,.662415777590,.657806693297,.653172842954
4520 DATA .648514401022,.643831542890,.639124444864,.634393284164,.629638238915
,.624359488142,.620057211763,.615231590581,.610382306276,.605511041404
4530 DATA .600616479384,.595699304492,.5907593701859,.585797857456,.580813958096
,.575308191418,.570780745887,.565731810784,.560661576197,.555570233020
4540 DATA .550457972937,.545324988422,.540171472730,.534997619887,.529803624686
,.524589682678,.519355990166,.514102744193,.508830142543,.503538383726
4550 DATA .498227666973,.492898192230,.487550150148,.482183772079,.476799230063
,.471396736826,.465976495768,.460538710958,.455033587126,.449611329655
4560 DATA .444122144570,.438616238539,.433033318653,.427555093430,.422000270800
,.416429560098,.410843171058,.405241314005,.399624199846,.393992040061
4570 DATA .388345046699,.382683432365,.377007410216,.371317193952,.365612997305
,.359395036535,.354163525420,.348418680249,.342660717312,.336889853392
4580 DATA .331106305760,.325310292162,.319502030316,.313681740399,.307849640042
,.302005949319,.296150888244,.290284677254,.284407537211,.278519689385
4590 DATA .272621355450,.266712757475,.260734117915,.254865659605,.248927605746
,.242980179903,.237023605994,.231058106281,.225063911360,.219101240157
4600 DATA .213110319916,.207111376192,.201104634842,.195090322016,.189063664150
,.183039887955,.177004220412,.170961388760,.164913120490,.158858143334
4610 DATA .152797185258,.146730474455,.140658239333,.134560708507,.128498110794
,.122410675199,.116318630912,.110222207294,.104121633672,.980171403296E-1
4620 DATA .919089564971E-1,.857973123444E-1,.796824379714E-1,.735645635997E-1,.
674439195637E-1,.613207363022E-1,.551952443497E-1,.490676743274E-1
4630 DATA .429382569349E-1,.368072229414E-1,.306748031762E-1,.245412285229E-1,.
184067299058E-1,.122715382857E-1,.613588464915E-2,0

```

TR 6533

```
4640 READ C(+)
4650 M=1024-N
4660 FOR I=0 TO N-4
4670 C(I+1)=C(M*I+1)
4680 NEXT I
4690 N1=N/4
4700 N2=N1+1
4710 N3=N2+1
4720 N4=N1+N3
4730 Log2n=INT(1.4427*LOG(N)+.5)
4740 FOR I1=1 TO Log2n
4750 I2=2^(Log2n-I1)
4760 I3=2*I2
4770 I4=N/I3
4780 FOR I5=1 TO I2
4790 I6=(I5-1)*I4+1
4800 IF I6<=N2 THEN 4840
4810 N6=-C(N4-I6)
4820 N7=-C(I6-N1)
4830 GOTO 4860
4840 N6=C(I6)
4850 N7=-C(N3-I6)
4860 FOR I7=0 TO N-I3 STEP I3
4870 I8=I7+I5
4880 I9=I8+I2
4890 N8=X(I8)-X(I9)
4900 N9=Y(I8)-Y(I9)
4910 X(I8)=X(I8)+X(I9)
4920 Y(I8)=Y(I8)+Y(I9)
4930 X(I9)=N6*N8-N7*N9
4940 Y(I9)=N6*N9+N7*N8
4950 NEXT I7
4960 NEXT I5
4970 NEXT I1
4980 I1=Log2n+1
4990 FOR I2=1 TO 10           ! 2^10=1024
5000 C(I2)=1
5010 IF I2>Log2n THEN 5030
5020 C(I2)=2^(I1-I2)
5030 NEXT I2
```

```

5040 K=1
5050 FOR I1=1 TO C(10)
5060 FOR I2=I1 TO C(9) STEP C(10)
5070 FOR I3=I2 TO C(8) STEP C(9)
5080 FOR I4=I3 TO C(7) STEP C(8)
5090 FOR I5=I4 TO C(6) STEP C(7)
5100 FOR I6=I5 TO C(5) STEP C(6)
5110 FOR I7=I6 TO C(4) STEP C(5)
5120 FOR I8=I7 TO C(3) STEP C(4)
5130 FOR I9=I8 TO C(2) STEP C(3)
5140 FOR I10=I9 TO C(1) STEP C(2)
5150 J=I10
5160 IF K>J THEN 5230
5170 A=X(K)
5180 X(K)=X(J)
5190 X(J)=A
5200 A=Y(K)
5210 Y(K)=Y(J)
5220 Y(J)=A
5230 K=k+1
5240 NEXT I10
5250 NEXT I9
5260 NEXT I8
5270 NEXT I7
5280 NEXT I6
5290 NEXT I5
5300 NEXT I4
5310 NEXT I3
5320 NEXT I2
5330 NEXT I1
5340 SUBEND
5350 !

5360 DEF FNArg(X,Y)           ! PRINCIPAL ARG(Z)
5370 IF X=0 THEN A=.5*PI*SGN(Y)
5380 IF X<>0 THEN A=ATN(Y/X)
5390 IF X<>0 THEN A=A+PI*<(I-2*(Y<0))
5400 RETURN A
5410 FNEND
5420 !

5430 SUB Data(N,X(*))
5440 OPTION BASE 1
5450 REDIM X(2,N)
5460 DATA 1,2,6,3,1,1,2,1,4,5,3,2,1,5,6,1,2,4,8,9
5470 DATA 2,1,0,1,5,3,0,1,2,6,2,2,4,2,3,5,6,9,8,2
5480 READ X(*)
5490 SUBEND

```

TR 6533

NUMBER OF DATA POINTS IN EACH PROCESS N = 20
MAXIMUM ORDER OF PREDICTIVE FILTER Pmax = 6
SIZE OF FFT Nfft = 256

PROCESS NUMBER 1

1 2 6 3 1 1 2 1 4 5 3 2 1 5 6 1 2 4 3 9

PROCESS NUMBER 2

2 1 0 1 5 3 0 1 2 6 3 2 2 4 2 3 5 6 9 8 2

MEANS OF INPUT DATA (Ave):

3.35

3.2

COVARIANCE MATRIX OF INPUT DATA (R):

.5.7275 .83

.83 6.16

AKAIKE INFORMATION CRITERION:

P	Aic(P)
0	.354363690E+01
1	.324147848E+01
2	.313209545E+01
3	.342425965E+01
4	.235777558E+01
5	.248589498E+01
6	.266117185E+01

.. .

Pbest = 4

Ub_{best}:

.54593344383 .226987553923

.226987553923 4.00240808163

FORWARD PARTIAL CORRELATION COEFFICIENTS:

P	Bp(1,1)	Bp(2,1)	Bp(1,2)	Bp(2,2)
1	.326847861E+00	-.296055028E-01	.433506958E+00	.492296101E+00
2	-.497079412E+00	.851055338E-01	.177974150E+00	-.275017512E+00
3	-.172083146E+00	.237335358E+00	.586121047E-01	.154803723E+00
4	-.143631688E+00	-.110686655E+00	.734743629E+00	-.124715363E+00
5	-.516644665E-01	-.440540782E+00	.193329089E+00	.883560194E+00
6	.901306062E-01	-.736616304E-01	-.256580155E+00	.734752737E+00

BACKWARD PARTIAL CORRELATION COEFFICIENTS:

P	Bp(1,1)	Bp(2,1)	Bp(1,2)	Bp(2,2)
1	.391694481E+00	.451665794E+00	-.139717614E-01	.427449481E+00
2	-.657848877E+00	.178422853E+00	.371402210E-01	-.192143512E+00
3	-.218767381E+00	.685350177E-01	.177465355E+00	.129759954E+00
4	-.128639908E+00	.100617477E+01	-.365534759E-01	-.944141856E-01
5	-.257137623E-01	.194124206E+00	-.219204303E+00	.117920510E+00
6	.182731463E+00	-.284468163E+00	.626220731E-01	.161491679E+00

FORWARD PREDICTIVE FILTER COEFFICIENTS FOR PDEST:

P	$A_p(1,1)$	$A_p(2,1)$	$R_p(1,2)$	$A_p(2,2)$
1	.235726249E+00	.174118149E+00	.296570575E+00	.670170572E+00
2	-.600483360E+00	-.164936772E+00	.4126994679E+00	-.442413930E+00
3	-.404360932E+00	.342089409E+00	-.235741642E+00	.251445573E+00
4	-.143631688E+00	-.1106866655E+00	.734742629E+00	-.124715363E+00

NORMALIZED CORRELATION MATRICES (Rn):

DELAY	AUTO11	CROSS12	CROSS12	AUTO22
0	.100000000E+01	.139734996E+00	.139734996E+00	.100000000E+01
1	.389669762E+00	.402437203E-01	.495250946E+00	.488307047E+00
2	-.284751305E+00	.912480910E-01	.511090660E+00	.648872368E-01
3	-.372945922E+00	.195208145E+00	.117107113E+00	.663026688E-01
4	-.223941701E-01	.876238663E-01	.190792716E+00	.100976458E+00
5	.396697360E+00	-.896791098E-01	.112701803E+00	.122691975E+00
6	.330388400E+00	-.836262522E-01	-.951969127E-01	.188386781E-01

SPECTRAL DENSITY MATRIX AND COHERENCE, FROM ZERO FREQUENCY - BIN 1):

BIN	AUTO11	AUTO22	RE(CROSS12)	IM(CROSS12)	MAG SO COH	ARGUMENT
1	.563234E-01	.130480E+00	.848704E-01	.600000E+01	.980117E+00	.000000E+01
2	.362462E-01	.130295E+00	.847113E-01	-.254607E-02	.980064E+00	-.300468E-01
3	.560152E-01	.129740E+00	.842359E-01	-.506953E-02	.979904E+00	-.601108E-01
4	.356327E-01	.128822E+00	.834493E-01	-.754840E-02	.979634E+00	-.902094E-01
5	.351025E-01	.127549E+00	.823603E-01	-.996105E-02	.979250E+00	-.120360E+00
6	.544301E-01	.125934E+00	.809811E-01	-.122673E-01	.978746E+00	-.150581E+00
7	.336226E-01	.123994E+00	.793277E-01	-.145063E-01	.978113E+00	-.180892E+00
8	.526890E-01	.121751E+00	.774195E-01	-.166075E-01	.977342E+00	-.211311E+00
9	.516400E-01	.119230E+00	.752793E-01	-.185704E-01	.976419E+00	-.241852E+00
10	.504882E-01	.116460E+00	.729330E-01	-.203857E-01	.975331E+00	-.272557E+00
11	.492475E-01	.113474E+00	.704088E-01	-.220448E-01	.974059E+00	-.303429E+00
12	.479335E-01	.110309E+00	.677369E-01	-.235426E-01	.972584E+00	-.334499E+00
13	.465623E-01	.107002E+00	.649485E-01	-.248774E-01	.970933E+00	-.365795E+00
14	.451507E-01	.103593E+00	.620751E-01	-.260508E-01	.968928E+00	-.39745E+00
15	.437158E-01	.100121E+00	.591473E-01	-.270676E-01	.966688E+00	-.429181E+00

116	.495654E-02	.527756E-02	.180088E-02	.366875E-02	.638529E+00	.111448E+01
117	.464126E-02	.492382E-02	.190282E-02	.323458E-02	.616259E+00	.103904E+01
118	.436922E-02	.461992E-02	.198172E-02	.284179E-02	.534614E+00	.961851E+00
119	.413522E-02	.435955E-02	.204244E-02	.246491E-02	.573915E+00	.882822E+00
120	.393482E-02	.413733E-02	.208889E-02	.215898E-02	.554351E+00	.801897E+00
121	.376422E-02	.394377E-02	.212416E-02	.185948E-02	.536176E+00	.719053E+00
122	.362025E-02	.379007E-02	.215073E-02	.158236E-02	.519605E+00	.634308E+00
123	.350027E-02	.365814E-02	.217053E-02	.132398E-02	.504935E+00	.547727E+00
124	.340211E-02	.355042E-02	.218509E-02	.108104E-02	.492036E+00	.459427E+00
125	.332403E-02	.346487E-02	.219558E-02	.850527E-03	.481358E+00	.369582E+00
126	.326465E-02	.339991E-02	.220289E-02	.629679E-03	.472923E+00	.278416E+00
127	.322295E-02	.335433E-02	.220767E-02	.415919E-03	.466828E+00	.196214E+00
128	.319821E-02	.332731E-02	.221037E-02	.206809E-03	.463144E+00	.932912E-01
129	.319001E-02	.331836E-02	.221125E-02	.000000E+01	.461911E+00	.000000E+01

TRAPEZOIDAL SUMS OF SPECTRA:

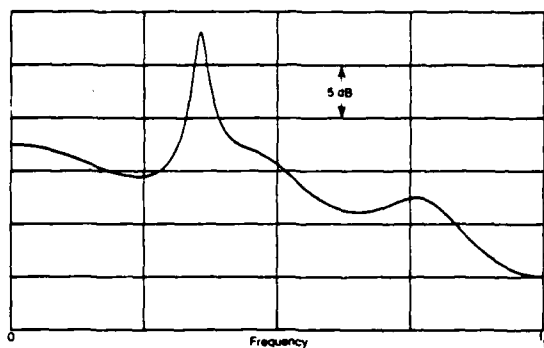
5.72678260464 6.15993376582 .630232954125

COVARIANCES OF INPUT DATA:

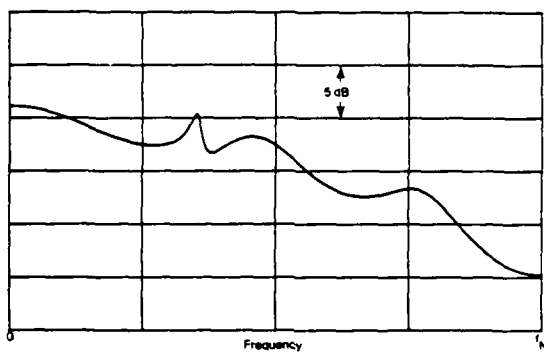
5.7275 6.16 .83

TR 6533

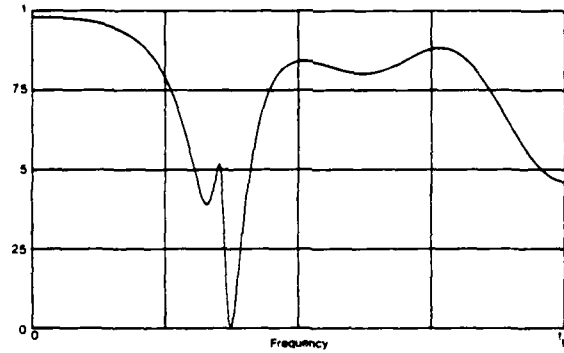
ALIASED NORMALIZED CORRELATION MATRICES:				
DELAY	AUTO11	CROSS21	CROSS12	AUTO22
0	.100000000E+01	.139783721E+00	.129783721E+00	.100000000E+01
1	.389662823E+00	.402483863E-01	.495316301E+00	.488307810E+00
2	-.284711075E+00	.912157098E-01	.511114181E+00	.640949626E-01
3	-.372868877E+00	.195185513E+00	.117074400E+00	.663147971E-01
4	-.223628311E-01	.876380084E-01	.190781841E+00	.100979179E+00
5	.396652516E+00	-.896408926E-01	.112729049E+00	.122684113E+00
6	.330310631E+00	-.836012969E-01	-.951530121E-01	.188794710E-01
7	-.345026269E-01	.609690818E-02	-.999179326E-01	-.796893320E-02
8	-.308860295E+00	.824851230E-01	.131798148E-01	.197442248E-01
9	-.262499156E+00	.629998356E-01	.116921946E+00	-.191113963E-01
10	.795870936E-01	-.238734308E-01	.105767456E+00	-.211019705E-01
11	.310325251E+00	-.669643776E-01	-.976171226E-01	.506845393E-02
12	.192490120E+00	-.429532422E-01	-.148398183E+00	.290497257E-01
13	-.123481195E+00	.241857986E-01	-.432258845E-01	.212691423E-01
14	-.294362011E+00	.638641478E-01	.104657992E+00	-.219543987E-01
15	-.128164922E+00	.302603975E-01	.123725501E+00	-.315105569E-01
**				
116	-.244194112E-02	.913297510E-03	.313869734E-02	-.782794525E-03
117	.270370651E-02	.703065771E-03	.135635926E-02	-.620489604E-03
118	.411244195E-02	-.122243230E-03	-.167393100E-02	.177358396E-03
119	.805212010E-03	-.344466456E-03	-.265889725E-02	.750518242E-03
120	-.280736944E-02	-.822305920E-03	-.764920706E-02	.519056852E-03
121	-.264738177E-02	-.179269851E-04	.172870237E-02	-.239248236E-03
122	.440106016E-03	.869991252E-03	.216369761E-02	-.719997787E-03
123	.238535013E-02	.101284633E-02	.329164628E-02	-.439526451E-03
124	.112686107E-02	.992673477E-04	-.164236260E-02	.286993480E-03
125	-.121802675E-02	-.105565279E-02	-.171669788E-02	.698618350E-03
126	-.151757804E-02	-.124026530E-02	-.421074185E-04	.378592478E-03
127	.306556500E-03	-.866410300E-04	.146460666E-02	-.330374132E-03
128	-.148247837E-02	.133650385E-02	.133650385E-02	-.690972582E-03



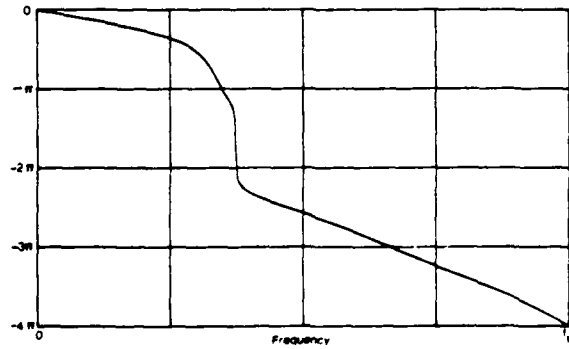
A-1A. Auto Spectrum of First Process



A-1B. Auto Spectrum of Second Process



A-1C. Magnitude-Squared Coherence



A-1D. Argument of Complex Coherence

Figure A-1. Spectral Estimates for N = 20, P_{max} = 6, P_{best} = 4

Appendix B

General Filter and Spectral Relations

For each integer k , let H_k be a rectangular matrix of (complex) constants, to be called the filter impulse response at delay $k\Delta$, where Δ is the time sampling increment. The number of filter outputs need not equal the number of filter inputs. For multichannel filter excitation W_n at time $n\Delta$, the filter output at time $n\Delta$ is given by the discrete convolution

$$X_n = \sum_k H_k W_{n-k} , \quad (B-1)$$

where the summation extends over all nonzero summands.

For a stationary excitation, let the correlation matrix of complex input process $\{W_n\}$ at delay $\ell\Delta$ be

$$\overline{W_n W_{n-\ell}^H} = P_\ell \quad (\text{non-diagonal matrix}), \quad (B-2)$$

where the overbar denotes an ensemble average, and the superscript H denotes a conjugate transpose. The z-transform of input correlation sequence $\{P_\ell\}$ is

$$Q(z) \equiv \Delta \sum_\ell z^{-\ell} P_\ell , \quad (B-3)$$

and the spectrum of input process $\{W_n\}$ is, for real frequency f ,

$$\begin{aligned} Q(f) &= Q(\exp(i2\pi f\Delta)) = \Delta \sum_\ell \exp(-i2\pi f\Delta\ell) P_\ell \\ &= \Delta \sum_\ell \exp(-iu\ell) P_\ell , \end{aligned} \quad (B-4)$$

where we let

$$u \equiv 2\pi f\Delta . \quad (B-5)$$

The correlation matrix of the filter output process $\{X_n\}$, at delay $\ell\Delta$, is given by using (B-1) and (B-2):

$$R_\ell \equiv \overline{X_n X_{n-\ell}^H} = \sum_{k,m} H_k \overline{W_{n-k}^H W_{n-\ell-m}^H} H_m^H = \sum_{k,m} H_k P_{\ell+m-k} H_m^H . \quad (B-6)$$

The z-transform of output correlation sequence $\{R_\ell\}$ is, by use of (B-6),

$$\begin{aligned}
 G(z) &\equiv \Delta \sum_{\ell} z^{-\ell} R_{\ell} = \Delta \sum_{\ell} z^{-\ell} \sum_{k,m} H_k P_{\ell+m-k} H_m^H \\
 &= \sum_k z^{-k} H_k \Delta \sum_{\ell} z^{-(\ell+m-k)} P_{\ell+m-k} \sum_m z^m H_m^H . \quad (B-7)
 \end{aligned}$$

Now define the z-transform of filter sequence $\{H_k\}$ by

$$H(z) = \sum_k z^{-k} H_k \quad (B-8)$$

and define the quantity

$$H^H(z) \equiv [H(z)]^H , \text{ including conjugation of } z. \quad (B-9)$$

Then

$$H^H\left(\frac{1}{z^*}\right) = \left[H\left(\frac{1}{z^*}\right)\right]^H = \left[\sum_k z^{*k} H_k\right]^H = \sum_k z^k H_k^H . \quad (B-10)$$

We now employ (B-8), (B-3), and (B-10) in (B-7) to obtain

$$G(z) = H(z) Q(z) H^H\left(\frac{1}{z^*}\right) . \quad (B-11)$$

The spectrum of output process $\{X_n\}$ is then, at real frequency f ,

$$\begin{aligned}
 G(f) &= G(\exp(i2\pi f\Delta)) = \Delta \sum_{\ell} \exp(-i2\pi f\Delta\ell) R_{\ell} \\
 &= H(f) Q(f) H^H(f) ,
 \end{aligned} \quad (B-12)$$

where we employed (B-11), (B-4), and set

$$H(f) = H(\exp(i2\pi f\Delta)) = \sum_k \exp(-i2\pi f\Delta k) H_k . \quad (B-13)$$

We also employed the property that

$$H^H(f) = [H(f)]^H = \sum_k \exp(i2\pi f\Delta k) H_k^H , \quad (B-14)$$

or

$$H^H \left(\frac{1}{\exp(-i2\pi f\Delta)} \right) = H^H(\exp(i2\pi f\Delta)) = H^H(f) . \quad (B-15)$$

Finally, from convolution (B-1), we obtain the z-transform of output data sequence $\{X_n\}$ as

$$X(z) \equiv \sum_n z^{-n} X_n = H(z) W(z) , \quad (B-16)$$

where we used (B-8) and defined

$$W(z) = \sum_n z^{-n} w_n . \quad (B-17)$$

The major results thus far are given by (B-1), (B-16), (B-11), and (B-12) for a general filter and excitation.

ARMA Process

For a multichannel, autoregressive, moving-average process, the recursion is given by

$$X_n = \sum_k E_k X_{n-k} + \sum_k F_k W_{n-k} . \quad (B-18)$$

The z-transform of this equation is

$$X(z) = E(z) X(z) + F(z) W(z) , \quad (B-19)$$

where

$$E(z) \equiv \sum_k z^{-k} E_k , \quad F(z) \equiv \sum_k z^{-k} F_k . \quad (B-20)$$

Then we can solve (B-19) for $X(z)$ as

$$X(z) = [I - E(z)]^{-1} F(z) W(z) = H(z) W(z) , \quad (B-21)$$

where the transfer function from input to output is

$$H(z) \equiv [I - E(z)]^{-1} F(z) \quad (B-22)$$

in terms of the parameters of recursion (B-18). But now (B-22) is in the framework of the presentation above; namely, the spectrum of output process $\{X_n\}$ is, from (B-12),

$$G(f) = H(f) Q(f) H^H(f) , \quad (B-23)$$

where

$$\begin{aligned} H(f) &= [I - E(f)]^{-1} F(f) , \\ E(f) &= E(\exp(i2\pi f\Delta)) = \sum_k \exp(-i2\pi f\Delta k) E_k , \\ F(f) &= F(\exp(i2\pi f\Delta)) = \sum_k \exp(-i2\pi f\Delta k) F_k . \end{aligned} \quad (B-24)$$

Example

As an example of (B-18), consider the multichannel first-order recursion

$$X_n = E_1 X_{n-1} + W_n \quad (B-25)$$

with the input spectrum for $\{W_n\}$,

$$Q(f) = \Delta I \quad \text{for all } f . \quad (B-26)$$

This is a white process, uncorrelated from channel to channel. Then

$$\begin{aligned} E(z) &= z^{-1} E_1 , \quad F(z) = I , \\ H(z) &= (I - z^{-1} E_1)^{-1} , \\ G(f) &= \Delta H(f) H^H(f) . \end{aligned} \quad (B-27)$$

Specialization to Two-Channel Process

We further specialize example (B-25) to the two-input, two-output channel process characterized by coefficient matrix

$$E_1 = \begin{bmatrix} a & b \\ c & d \end{bmatrix} \quad (\text{complex coefficients}). \quad (B-28)$$

Then (B-27) and (B-22) yield transfer function

$$\begin{aligned}
 H(z) &= \begin{bmatrix} 1 - z^{-1}a & -z^{-1}b \\ -z^{-1}c & 1 - z^{-1}d \end{bmatrix}^{-1} \\
 &= \frac{1}{1 - z^{-1}(a + d) + z^{-2}(ad - bc)} \begin{bmatrix} 1 - z^{-1}d & z^{-1}b \\ z^{-1}c & 1 - z^{-1}a \end{bmatrix}. \quad (\text{B-29})
 \end{aligned}$$

There follows

$$\begin{aligned}
 H^H(1/z^*) &= [H(1/z^*)]^H \\
 &= \frac{1}{1 - z(a + d)^* + z^2(ad - bc)^*} \begin{bmatrix} 1 - zd^* & zc^* \\ zb^* & 1 - za^* \end{bmatrix}. \quad (\text{B-30})
 \end{aligned}$$

and

$$\begin{aligned}
 G(z) &\equiv H(z) H^H(1/z^*) \equiv \begin{bmatrix} g_{11}(z) & g_{12}(z) \\ g_{21}(z) & g_{22}(z) \end{bmatrix} \\
 &= \frac{1}{D} \begin{bmatrix} 1 + |b|^2 + |d|^2 - z^{-1}d - zd^* & -a^*b - c^*d + z^{-1}b + zc^* \\ -ab^* - cd^* + z^{-1}c + zb^* & 1 + |a|^2 + |c|^2 - z^{-1}a - za^* \end{bmatrix}, \quad (\text{B-31})
 \end{aligned}$$

where

$$D = \left[1 - z^{-1}(a + d) + z^{-2}(ad - bc) \right] \left[1 - z(a + d)^* + z^2(ad - bc)^* \right]. \quad (\text{B-32})$$

Inspection of denominator D in (B-32) reveals that $G(z)$ has poles (i.e., all the elements of matrix $G(z)$ have poles) at

$$z_{\infty} = \frac{a + d \pm \sqrt{(a + d)^2 - 4(ad - bc)}}{2} \quad (B-33)$$

and at

$$\frac{1}{z_{\infty}^*} = \frac{1}{|z_{\infty}|} \exp(i \arg(z_{\infty})) . \quad (B-34)$$

That is, even though recursion (B-25) is limited to first-order regressive and white independent excitations (see (B-26)), $G(z)$ has *four* poles in the finite z -plane. Generally, if $H(z)$ has a pole at z_{∞} , then $H(1/z^*)$ has a pole at $1/z_{\infty}^*$; so if

$$z_{\infty} = r \exp(i\theta), \quad \text{then} \quad 1/z_{\infty}^* = \exp(i\theta)/r \quad (B-35)$$

has the same argument.

In addition, element $g_{11}(z)$ in (B-31) has a zero at ∞ and three zeros in the finite z -plane, at

$$z_0 = 0 \quad \text{and} \quad z_0 = \frac{1 + |b|^2 + |d|^2 \pm \sqrt{(1 + |b|^2 + |d|^2)^2 - 4|d|^2}}{2d^*} \quad (B-36)$$

The product of the latter two zero locations is $d/d^* = \exp(i2\arg(d))$. Thus, the auto spectrum of process 1 has three zeros and four poles, even though the multichannel recursion, (B-25), is first-order regressive. Similar behavior is true of the auto spectrum of the second process, as well as the cross spectrum between the two processes.

The magnitude-squared coherence for this example is, from (B-31) and (B-5),

$$\begin{aligned} & \frac{g_{12}(\exp(iu)) g_{21}(\exp(iu))}{g_{11}(\exp(iu)) g_{22}(\exp(iu))} \\ &= \frac{| -a^*b - c^*d + b \exp(-iu) + c^* \exp(iu) |^2}{[|1 - d \exp(-iu)|^2 + |b|^2] [|1 - a \exp(-iu)|^2 + |c|^2]} . \end{aligned} \quad (B-37)$$

This has four zeros and four poles in the finite z -plane.

Numerical Example

We now specialize (B-28) to example (6) in the main text:

$$E_1 = \begin{bmatrix} a & b \\ c & d \end{bmatrix} = \begin{bmatrix} .85 & -.75 \\ .65 & .55 \end{bmatrix} . \quad (B-38)$$

The four poles of the spectrum $G(z)$ are located at

$$z_{\infty} = .7 \pm i .6819 , \quad 1/z_{\infty}^* = .7330 \pm i .7140 , \quad (B-39)$$

and the zeros of $g_{11}(z)$ are z^*

$$z_0 = 0 , \quad 3.0646 , \quad .3263 , \quad \infty . \quad (B-40)$$

The zeros of $g_{12}(z)$ are located instead at

$$z_0 = 0 , \quad .8802 , \quad -1.3109 , \quad \infty . \quad (B-41)$$

The magnitude-squared coherence simplifies to

$$\frac{1.0634 - .056 \cos(u) - .975 \cos(2u)}{[1.865 - 1.1 \cos(u)] [2.145 - 1.7 \cos(u)]} . \quad (B-42)$$

This example was used frequently in the main body of this report. The peak value is .9990128 at $u = .772564$, or $2f\Delta = .245915$.

References

1. J.P. Burg, "A New Analysis Technique for Time Series Data," *NATO Advanced Study Institute on Signal Processing*, Enschede, Netherlands, vol. 1, August 1968.
2. R.T. Lacoss, "Data-Adaptive Spectral Analysis Methods," *Geophysics*, vol. 36, no. 4, August 1971, pp. 661-675.
3. J. Makhoul, "Linear Prediction: A Tutorial Review," *Proceedings of the IEEE*, vol. 63, no. 4, April 1975, pp. 561-580.
4. A.H. Nuttall, "Spectral Analysis of a Univariate Process with Bad Data Points, via Maximum Entropy and Linear Predictive Techniques," NUSC Technical Report 5303, 26 March 1976.
5. S.L. Marple, "A New Autoregressive Spectrum Analysis Algorithm," *IEEE Trans. on Acoustics, Speech, and Signal Processing*, vol. ASSP-28, no. 4, August 1980, pp. 441-454.
6. A.H. Nuttall, "Application of Linear Predictive Spectral Analysis to Multiple Tones in Noise," NUSC Technical Memorandum 791218, 12 December 1979.
7. A.H. Nuttall, *FORTRAN Program for Multivariate Linear Predictive Spectral Analysis, Employing Forward and Backward Averaging*, NUSC Technical Document 5419, 19 May 1976.
8. A.H. Nuttall, *Multivariate Linear Predictive Spectral Analysis, Employing Weighted Forward and Backward Averaging: A Generalization of Burg's Algorithm*, NUSC Technical Report 5501, 13 October 1976.
9. A.H. Nuttall, *Positive Definite Spectral Estimate and Stable Correlation Recursion for Multivariate Linear Predictive Spectral Analysis*, NUSC Technical Report 5729, 14 November 1977.
10. S.L. Marple, personal communication.

Initial Distribution List

Addressee	No. of Copies
ASN (RE&S)	1
OUSDR&E (Research & Advanced Technology)	2
Deputy USDR&E (Res & Adv Tech)	1
OASN	1
ONR, ONR-100, -200, -102, -222, 486	5
CNO, OP-098, -96	2
CNM, MAT-08T, -08T2, SP-20	3
DIA, DT-2C	1
NAV SURFACE WEAPONS CENTER, White Oak Laboratory	1
NRL	1
NRL, USRD	1
NORDA (Dr. R. Goodman, 100)	1
USOC, Code 241, 240	2
SUBASE LANT	1
NAVSUBSUPACNLON	1
OCEANAV	1
NAVOCEANO, Code 02	1
NAVELECSYSCOM, ELEX 03	1
NAVSEASYSCOM, SEA-003	1
NAVAL SEA SYSTEM DETACHMENT, Norfolk	1
NASC, AIR-610	1
NAVAIRDEVVCEN	1
NOSC	1
NOSC, Code 6565 (Library)	1
NAVWPNSCEN	1
DTNSRDC	1
NAVCOASTSYSLAB	1
CIVENGRLAB	1
NAVSURFWPNCEN	1
NUWES, San Diego	1
NUWES, Hawaii	1
NISC	1
NAVSUBSCOL	1
NAVPGSCOL	1
NAWWARCOL	1
NAVTRAEEQUIPCENT (Technical Library)	1
APL/UW, Seattle	1
ARL/Penn State, State College	1
Center for Naval Analyses (Acquisition Unit)	1
DTIC	2
DARPA	1
NOAA/ERL	1
National Research Council	1

Initial Distribution (Cont'd)

Weapon System Evaluation Group	1
Woods Hole Oceanographic Institute	1
ARL, Univ of Texas	1
Marine Physical Lab, Scripps	1
Dr. David Middleton, 127 East 91st St., New York, NY 10028	1
Bolt, Beranek, and Newman, Cambridge, MA (Herbert Gish)	1
Bolt, Beranek, and Newman, Canoga Park, CA (Dr. Allan G. Piersol)	1
Colorado State University (Prof. Louis Scharf)	1
University of Rhode Island (Prof. Donald Tufts)	1
Nat. Def. Res. Org. (C. van Schooneveld)	1
The Analytic Sciences Corp. (Dr. S. L. Marple)	1
Gould Inc. (T. E. Barnard, P. F. Lee)	2
Yale University (Prof. P. M. Schultheiss)	1
Royal Military College (Prof. Y. T. Chan)	1
University of Florida (Donald G. Childers)	1
Diagnostic Retrieval Systems (Jack Williams)	1

**DATE:
ILME**